NUMERICAL MODELLING FOR STRESSES IN RAILWAY SUBGRADE WITH GEOCELL CONFINED BALLAST

A DISSERTATION
SUBMITTED IN PARTIAL FULFILLMENT OF THE REQUIREMENTS
FOR THE AWARD OF THE DEGREE
OF

MASTER OF TECHNOLOGY
IN
GEOTECHNICAL ENGINEERING

Submitted by:
AMNINDER SINGH NAYYAR
2K17/GTE/04

Under the supervision of

Prof. ANIL KUMAR SAHU

DEPARTMENT OF CIVIL ENGINEERING
DELHI TECHNOLOGICAL UNIVERSITY
(Formerly Delhi College of Engineering)
Bawana Road, Delhi-110042

JULY 2019

DEPARTMENT OF CIVIL ENGINEERING

DELHI TECHNOLOGICAL UNIVERSITY

(Formerly Delhi College of Engineering)

Bawana Road, Delhi-110042

CANDIDATE'S DECLARATION

I, Amninder Singh Nayyar (2K17/GTE/04) of M.Tech (Geotechnical Engineering), hereby declare that the Project Dissertation titled " NUMERICAL MODELLING FOR STRESSES IN RAILWAY SUBGRADE WITH GEOCELL CONFINED BALLAST " which is submitted by me to the Department of Civil Engineering, Delhi Technological University, Delhi is submitted in partial fulfillment of the requirement for the award of the degree of Master of Technology, is original and not copied from any source without proper citation. This work has not previously formed the basis for the award of any Degree, Diploma Associateship, Fellowship or other similar title or recognition.

Place: Delhi **(AMNINDER SINGH NAYYAR)**

Date: **2K17/GTE/04**

DEPARTMENT OF CIVIL ENGINEERING

DELHI TECHNOLOGICAL UNIVERSITY

(Formerly Delhi College of Engineering)

Bawana Road, Delhi-110042

CERTIFICATE

I hereby certify that the Project Dissertation entitled " NUMERICAL MODELLING FOR STRESSES IN RAILWAY SUBGRADE WITH GEOCELL CONFINED BALLAST" which is submitted by Amninder Singh Nayyar (2K17/GTE/04) of M.Tech (Geotechnical Engineering), Delhi Technological University, Delhi submitted in partial fulfillment of the requirement for the award of Master of Technology, is a record of the project work carried out by the student under my supervision. To the best of my knowledge, this work has not been submitted in part or full for any Degree or Diploma to this University or elsewhere.

Place: Delhi
Date:

(Prof. ANIL KUMAR SAHU)
SUPERVISOR & PROFESSOR
Department of Civil Engineering

ACKNOWLEDGEMENT

As I write this acknowledgement, I must clarify that this is not just a formal acknowledgement but also a sincere note of thanks and regard from my side. I have taken efforts in this Project Dissertation. However, it would not have been possible without the kind support and help of many individuals and organizations. I would like to extend my sincere thanks to all of them. I express my sincere thanks to the University Management. My sincere thanks also go to Vice Chancellor Prof. Yogesh Singh and Head of Department Prof. Nirendra Dev. I am highly indebted to my supervisor Prof. Anil Kumar Sahu for his guidance and constant supervision as well as for providing necessary information regarding the project & also for his support in completing the Project Dissertation. I would like to express my special gratitude and thanks to Prof. A. Trivedi, Prof. A.K Shrivastava, Prof. K.C. Tiwari, Prof. A.K. Gupta, Prof. Naresh Kumar, Department of Civil Engineering and all the Faculty member of Civil Engineering Delhi Technological University for guiding throughout this project. I would also like to thanks Prof. Vijay Gautam for taking pain to help me understand the software Abaqus/CAE. My thanks and appreciations also go to my colleague in developing the project and people who have willingly helped me out with their abilities. In the end, I thank god almighty and my parents for bestowing their blessings and grace in completion of the Project Dissertation.

AMNINDER SINGH NAYYAR
2K17/GTE/04
Department of Civil Engineering
Delhi Technological University

ABSTRACT

With the improvement in railway infrastructure, hauling capacity and speed of trains have increased. Due to this, there have been an increase in overall stresses throughout the railway substructure. In order to overcome this, various improvement techniques are being analysed. One of the improvement techniques is to confine the ballast using geocell. The decrease in subgrade stresses has been assumed to occur as a result of geocell inclusion. For the validation of this assumption, numerical modelling has been done in 2-D and 3-D, respectively. The results have shown that with the inclusion of geocell confinement and with an increase in its width, subgrade stresses have decreased. Also, it have been observed at greater width, stresses on ballast embankment slope have increased drastically. Graphical Trends of results have been found similar on comparing the 3-D and 2-D analyses results, but the difference in magnitude is high. More reliable results are observed in 3-D analysis as a 3-D models have been solved as slab instead of a beam as in case of 2-D analyses. Also, from whole analyses optimum confinement width has been determined.

CONTENTS

LIST OF FIGURES

LIST OF TABLES

LIST OF SYMBOLS AND ABBREVIATIONS

ABC ICF	Airconditioned Buffet Coach Integral Coach factory.
CAE	Complete Abaqus Environment.
CBC IRS	Central Buffer Couplers Indian Railway Standards.
C3D10I	10-node general purpose tetrahedron with improved surface stress formulation.
C3D4	A 4-node linear tetrahedron.
C3D8R	An 8-node linear brick, reduced integration, hourglass control.
CPE6M	A 6-node modified quadratic plane strain triangle.
CPE4R	A 4-node bilinear plane strain quadrilateral, reduced integration, hourglass control.
CPE8R	An 8-node biquadratic plane strain quadrilateral, reduced integration.
FE	Finite Element
kg	Kilogram
km	Kilometre
kN	Kilonewton
M	Metre
MPa	Megapascal
NPA	Novel Polymeric Alloy
Pa	Pascal
psi	Pounds per square inch
PCS	Prestressed Concrete Sleeper
sec	Seconds
SF	Speed Factor

WDM_4	Wide-gauge Diesel-fuelled Mix-load Class 4.
WDM_2	Wide-gauge Diesel-fuelled Mix-load Class 2.
WDM_1	Wide-gauge Diesel-fuelled Mix-load Class 1.
WP(CLW)	Wide-gauge Passenger (Chittaranjan Locomotive Works).

CHAPTER 1

INTRODUCTION

Railway Transport System is one of the greatest inventions of the 19th century. With this invention transportation system has been revolutionized as it results in faster and economical movement of people and goods. With India's GDP growth rate 6-8%, transport needs of both people and goods have increased, and the railway being the economics one needs to be strengthened. Various high-speed train projects have been announced which includes the bullet trains from Ahmedabad and Mumbai. For this purpose, rail technology has to be improved.

In the case of a high-speed train, railway operation quality depends on geotechnics. Combination of railway engineering and geotechnical engineering results in Railway Geotechnics. Railway Geotechnics consists of the track, track substructure, load environment, mechanics, design, material selection, construction, measurements and management.

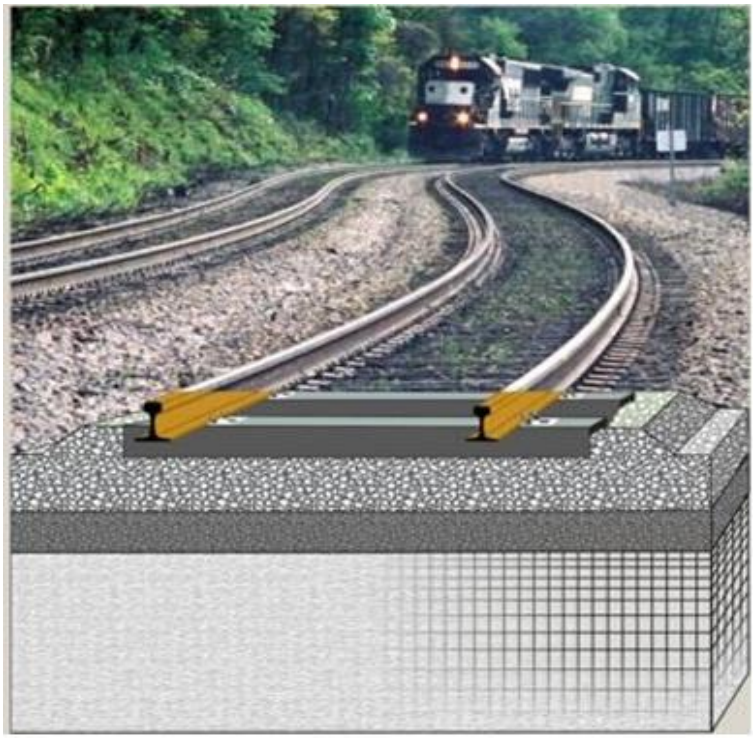

Figure 1.1 Pictorial representation of Rail-Geotechnics Components (Li et al. 2015)

Study of railway geotechnics includes various methods of improving the parametric properties of its components.

1.1 COMPONENTS OF RAILWAY GEOTECHNICS

Various components of railway geotechnics are –

1.1.1 Rail

1.1.2 Sleeper

1.1.3 Ballast

1.1.4 Subgrade

1.1.1 Rail

Rail is that component of the Rail system which is in direct contact with the train wheels. It consists of Head, Web and Foots. Double-headed, bull-headed and flat-footed are the type of rails, but the performance of flat-footed rail is much better than the others. Strength of rail section is represented by the modulus of the section. Figure 1.3 shows the type of rails.

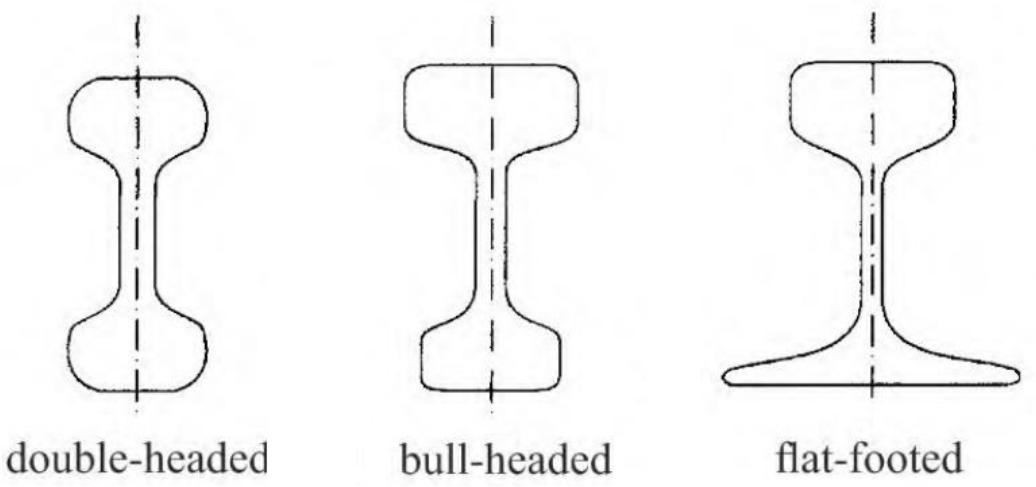

Figure 1.2 Types of Rails (Mundrey 2010)

Functions of Rail: -

- Provides hard and unyielding surface to rolling wheel.
- Provides a smooth surface (to keep the friction between the rails and wheels minimum).

- Act as a beam and transmit the wheel loads to the sleepers.

1.1.2 Sleeper

Sleeper is the component which lies in between the rail and ballast. Following are the materials used for make different type of sleeper used in India Railway: -

- Wooden
- Cast iron
- Concrete
- Steel

Most commonly used, in modern Indian railway, are Concrete type.

Functions of Sleeper are the following: -

- Transfering the load from rails to ballast uniformly.
- Acts as an elastic medium which absorbs blows and vibration caused due to moving train loads.
- Act as rigid support to rails.

The number of sleepers per unit rail length is defined by term sleeper density.

1.1.3 Ballast

Ballast is the material, granular in nature, placed above subgrade and is that layer which is in direct contact of sleeper ties. It is angular big size granular material obtained by crushing of rocks like basalt and granite. The thickness of ballast should be kept at least 200mm

Different types of ballast used in India are –

- Broken Stone
- Gravel
- Kankar
- Brick Ballast etc.

Functions of Ballast –

- Supports the sleepers.
- Transmits the train stresses over the subgrade uniformly.
- Maintaining proper drainage in tracks.
- Provide elasticity to the track.
- Used in boxing the sleeper for the lateral stability

1.1.4 Subgrade

Subgrade acts as a platform on which rail substructure lies. Subgrade can be natural soil or rock or compacted soil fill. Trackbed, Rail Foundation are other terms used for it. The primary function of the subgrade is to provide uniform and adequate support to the rail track system. Sometimes natural soil as subgrade is not adequate in that case either it is replaced by stiff soil. In some cases, reinforcement of ballast or subgrade is done in such a way that subgrade stress is decreased.

In present times, India is developing at a rapid rate. Along with India, Indian Railway is also evolving at a higher growth rate than ever. Development of Indian Railway includes traffic management of trains, infrastructural development of the railway station and the most important of all average speed of trains. Various high-speed train projects are under construction, and also the new railway track system components which are adequate for the stresses of the high-speed train are being constructed. One of the latest additions to components is Subgrade which results in the conception of another division Railway Geotechnics. Railway Geotechnics is a fusion of Railway Engineering and Geotechnical Engineering.

In many cases during the laying of new track system, Engineers faces the situation where the subgrade below the ballast is weak soil like soft clay. Soil improvement by replacement it with stiff and stable soil economic up to certain depth after which excavation is not a cost-effective option. In this type of situations, another option is to reinforce the soil or ballast with geosynthetics.

1.2 GEOCELL

Geocells are 3-D honeycombed structures, cellular in nature that result in a confining system when compacted soil is filled in its cells. They are also known as Cellular Confinement Systems. Polymeric materials cut into strips and joined together using ultrasonic welding in series result in Geocell. These strips of geocell when expanded form the stiff walls of a flexible 3D cellular mattress. Filling it with any material, the cell-material interaction occurs resulting in a new entity.

Functions of Geocell –

- Cellular confinement provided by it results in a reduction of soil particles lateral movements.
- It forms a stiffened entity, distributing loads over a larger area.

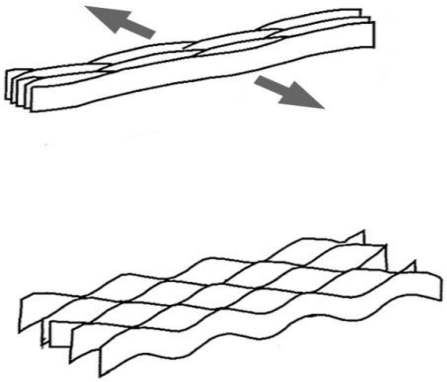

Figure 1.3 Geocell, when shipped (top) and outstretched (bottom) (Koerner, 2005)

Geocell is generally used in slope stability and earth retaining applications. With an increase in technology, advanced polymer manufactured using materials Novel Polymeric Alloy (NPA) is used to manufacture geocell, this geocell due to long life, higher stiffness and creep resistance are used in road and rail load support.

1.3 OBJECTIVES

Based on the literature survey in the field of railway geotechnics and geosynthetic reinforcements, the following objectives are to be performed –

- To perform stress analyses of railway subgrade with geocell confined ballast by analysing 2-D finite element model using Abaqus/CAE.
- To perform stress analyses of railway subgrade with geocell confined ballast by analysing 3-D finite element model using Abaqus/CAE.
- To compare the results of both 2-D and 3-D models.
- To determine the optimum geocell confinement width.

In order to fulfil the objectives, the literatures have been reviewed, further which is presented in the succeeding chapters.

CHAPTER 2

LITERATURE REVIEW

In the present chapter, literature has been reviewed with respect to the following aspects–

1) Numerical and physical modelling on railway geotechnics.
2) Static & dynamic analysis of some components of railway geotechnics.
3) The confinement of ballast and subgrade by geocell or similar materials

Cowland et al. (1993) monitored a geocell mattress foundation instrumentally and observed its performance using various instruments like surface settlement markers etc. Geocell used was formed from high-density polyethylene geogrids and has a triangular shaped cell. Embankment used for this monitoring, was of soft clay, was fully equipped with these instruments. From this whole monitoring, the conclusion was made that geocell mattress acts as a foundation (raft) to the embankment.

Yetimoglu et al. (1994) had done both numerical and physical modelling of rectangular footing on geogrid reinforced sand. For physical modelling, bearing capacity setup was prepared which consists of 70cm×70cm×100cm steel tank in which sand is placed and load is applied using a hydraulic pump, and for numerical, a finite element program DASCAR was used. Series of discrete shell element which were axisymmetric was used to represent geogrid reinforcement, footing and assembly of triangular and quadrilateral elements for sand, also axisymmetric. For reinforcement purpose, uniaxial geogrid was used. Results from both analyses were almost same suggesting that reinforced soil so increased bearing capacity, settlement corresponding to a load decreases, also he found that on increasing reinforced layer in sand properties of soil were improved and improvement was inversely proportional to vertical spacing between the layers.

Rajagopal et al. (1998) studied the effect of confinement due to geocell on the strength and stiffness of soils granular in nature. For this study, several triaxial compression tests were done. The geocells used for confinement were hand fabricated and material used were different woven and nonwoven geotextiles. The model geocells were designed using different types of geosynthetics and various mesh elements. The geocell-sand composites are of 200 mm in height and 100 mm in diameter. A triaxial test apparatus was used performed and different confining pressure. From results, the conclusion was made that apparent cohesive strength even to cohesionless soils is added due to geocell confinement. This apparent strength depends on the tensile modulus of the geosynthetic used to form the geocell.

Chaney et al. (2000) conducted an experimental study for evaluation of elastic modulus of geogrid-reinforced sand. Plate load tests were performed on sand reinforced at different

depths. From the deformation vs applied pressure graphs, it was concluded that deformation per unit pressure decreases in reinforced soil. Also, the data analysis of test result discerns the phenomenon of increment of elastic modulus with the addition of geogrid reinforcement.

Han and Gabr (2002) had compared the unreinforced pile-supported structure and reinforced pile-supported structure for supporting superstructure over soft soil. FLAC was used for numerical modelling of a non-linear hyperbolic elastic model. FLAC is a continuum model that uses an explicit finite difference code that is good at modelling large displacements. From the results, it was interpreted that presence of geosynthetics in the fill improves the stress concentration ratio, diminish the soil yield above pile head and decrease the chances of differential settlement as in ideal case geosynthetic reinforced soil is rigid. Also, the settlement minimises with an increase in tensile strength of the geosynthetics upto a limit of 4000kN/m, but beyond this, there is a very minimal effect.

Indraratna et al. (2006) demonstrated two different techniques of stabilising railroad bed. One was to reinforce ballast by geocomposites and others to reinforce the soft soil by prefabricated vertical drains. Purpose of ballast is to distribute the load uniformly form sleepers, damping of dynamic loads and proving free drainage condition. Ballast fails when it degrades and settles more. To reduce degradation, a uniformity coefficient of 2.2 for ballast material was recommended. For Settlement, geotextiles, geogrid and geocomposites were used, and modelling was done using PLAXIS, which is a finite element software and results got better in the same order. Also, the optimum depth for placing geosynthetics was 150mm. For improving soil PVDs were used. Shorts PVDs (5m-8m) were enough to release the pore pressure stiffness the foundations up to the depth of some metres.

In other research, Indraratna et al. (2006) conducted a large scale triaxial test to study the behaviour of ballast due to the application of static and dynamic loads. Effect of geosynthetics on the performance of ballast under similar loading condition was also investigated. A prismoid triaxial apparatus of large scale i.e. 800mm in length, 600mm width and 600mm in height was used for simulation of the real situation of railway track, and the load was provided with the help of servo-hydraulic actuator (cyclic vertical load). Fresh and Recycled ballast (dry and wet) was used, and for reinforcement purpose geotextile, geogrid and geocomposites were used. Results obtained after 500000 load cycles show a decrease in a settlement in reinforced soil. Least settlement was seen in case of geogrid. A similar pattern was followed in the case of lateral and vertical strain. Also, recycled ballast consisting of geocomposites results in a reduction in the breakage index as compared to the fresh unreinforced ballast.

Zhou and Wen (2006) conducted a laboratory test for the analysation of the effect layer of geosynthetic materials placed in a sand cushion, creating a composite layer over foundation composed of soft soil. All in-situ conditions of the embankment were simulated in the laboratory test. From the results, an observation was made that provision

of a geosynthetic material layer in embankment increase the overall bearing capacity and reduces the settlement of soft under the soil.

Lackenby et al. (2007) performed cyclic triaxial tests for the determination of the effects of confining pressure and deviator stress on deformation of ballast (permanent and resilient) and degradation. For having actual load condition, large scale triaxial apparatus was incorporated. Initially, the static load was applied, but after some time, the dynamic load was applied to replicate the high-speed load. From the test results, graphs were plotted between axial strain vs confining stress and BBI vs confining stress and conclusion was made that as confining pressure increase, axial strain decreases. Also confining pressure plays an essential role in ballast degradation.

Atalar et al. (2009) observed the effect of soil-geogrid composite on the young's modulus of elasticity of soil which is granular in nature with the help of cyclic plate load test. Elastic Modulus values were determined for the various arrangement of geogrid reinforcements. Three tests were conducted with a different number of reinforced layers. Reinforcement of soil was done using Bi-axial polymer geogrid (polypropylene). From the test, results conclusion was made that soil reinforced with geogrid shows improvement in various properties of soil. Out of which stiffness plays important role in predicting the strength of the soil. As stiffness is increased the settlement decreases. Increment in stiffness also means modulus of elasticity is increased. Modulus of elasticity improves from 9% to 54% increases with the increase in the reinforced layer. For determination of elastic modulus, cyclic plate load test equation is used.

Ziaie (2011) performed a laboratorial study of the outcomes of geogrid and geosynthetic reinforcement on the thickness of sub-base of the two-layer soil system. Bearing ratio test in four conditions- unreinforced, reinforced with sub base thickness 40,55 and70mm were performed. Two layers of soil are of sand(top) and clay (bottom). Soil classification was done according to the Unified Soil Classification system. Series of bearing ratio tests were conducted on oven-dried samples with the required amount of water content. Testing was done according to ASTM D1883-05. Results show that improvement in geogrid is more than geosynthetic reinforced and layer 40mm shows most the improvement while in 70mm layer improvement was negligible. It was concluded that less is the thickness of subbase more is the improvement, which benefits the requirement of decrease thickness of sub-base.

Leshchinsky and Ling (2013) suggests that in various case of railway geotechnics where ballast is inadequate for stress to be applied and improvement of below soil is expensive, in these cases geocell reinforcement of ballast should be done, in which ballast is confined in geocell which result in mattressing effect. For numerical modelling, approach has been used and for that purpose ABAQUS has been used. Ballast was modelled in such way that its obeyed Drucker Prager yield criterion. Geocell was modelled as elastic materials. FE mesh for ballast is represented as C3D4R, rails as C3D8R and soil as C3D8R. He further has done the numerical analysis on two basis- varying stiffness of geocell and varying stiffness of soil, comparing the subgrade stress. The conclusion made from results

of Abaqus were Confinement of ballast decrease the vertical deformation and settlement because of the mattressing effect in which geocell redistributes the stress in more uniform way. Also, peak stresses in very weak clay are reduced. Lateral deformation at ballast level is decreased. While modelling was done without taking time-dependent soil behaviour.

Kumar (2014) conducted a numerical analysis of statically and dynamically loaded pre-stressed concrete sleepers using ANSYS. For a better understanding of the dynamic effect on the sleeper comparison of finite element model with ballast and without ballast were compared. Dynamic analyses were done for the two conditions, free-free condition and in-situ condition and observation were made that in case free-free condition natural frequency was much lower than in case of the in-situ condition. The natural frequency and vibration mode shape of prestressed concrete sleepers highly depends on in-situ-condition.

Fu and Zheng (2014) created a 3-D FE model to investigate the track ground system for its dynamic behaviour when loads act on it due to high speed moving rail loads. For analysis purpose, finite element software ABAQUS was used to simulate the effect of high-speed trains on the track system. In ABAQUS, the model was designed using 8-noded solid element simulating rail system. The model contains rails, sleepers, ballast, embankment and was of 130m length. The parameter used to define these materials were, Poisson's ratio (μ), elasticity modulus (E) , density (γ) and, Shear (V_s) and Rayleigh (V_r) velocity. For dynamic purposes, it was assumed that X and Z direction boundaries would represent boundaries to absorb S and P waves. From a dynamic analysis, a conclusion was made that vertical displacement and velocity decreases with an increase in Young's modulus of ballast. Similarly, reduction of 26% in peak displacement was observed for high stiffness fill (10000MPa) and 15% were medium stiffness fill (1000MPa) was achieved at a point near the track centre in comparison to low stiffness soil (90.75MPa). This was also noticed that 20t axle load gives 25% more vertical displacement when compared to 15t axle load. However, these results don’t have practical validations.

Leshchinsky et al. (2015) conducted a number of triaxial compression test for the determination of mechanical property of sand (GP) mix with a microgrid. Use of microgrid grids results in an economic reinforced layer. Sand used was subangular and poorly graded while microgrid reinforcements have a composition of non-ceasing charcoal flexible fibreglass material. Microgrids of different aspect ratio and dimensions were used and orientation at which it was placed was random. A series of CD Triaxial Test were conducted, and from results, an increase in the angle of friction and modulus of elasticity was interpreted and were represented by strength improvement factor and stiffness improvement factor. It was also observed the reinforcement of greater aspect ratio at lesser concentration gives a better result than a higher concentration of reinforcement in soil. From the result, it was concluded that microgrid is cost effective method but may be sufficient for only shallow ground improvements.

Nikraz et al. (2015) used a method for calculate the load bearing behaviour of strip footing by software Abaqus/CAE.Soil behaviour in this software was represented by elasto-plastic Drucker-Prager model and footing and soil was assumed isotropic and linear elastic. Drucker-Prager model uses properties like density, modulus of elasticity, Poisson's ratio, cohesive strength, angle of friction (Φ) and dilation angle. Axi-symmetric approach was used to design the model. From the results of ABAQUS, it was concluded that for FEM analysis, the values of bearing capacity when dilation angle is considered is 13% higher than when dilation angle is considered and Terzaghi results and in between them. The model described in this paper is for short term stability of footing.

Van Dyk et al. (2015) evaluated the effectiveness of various methods of defining dynamic wheel load design factor to consider the dynamic effect while doing static analysis. Various evaluated were Talbot, Indian Railways, German Railways, British Railways etc. These methods for defining the dynamic factor considers various design elements- train speed, wheel diameter, track modulus, curve radius and other design elements. The conclusion from the study was made that higher no of elements considered while determining the dynamic factor better would be the dynamic representation dynamic load effect.

Das (2016) has reviewed different publishing and various case studies of different layers of ballast reinforced with geogrid on soft soil subgrade. Various reinforcement mechanism, the performance of geogrid reinforced ballast, the basis for selection of optimum geogrid, the influence of its stiffness etc. were assessed. The conclusion from the assessment was made that reinforcement of railroad bed with geogrid reduces the rate of permanent settlement. With an increase in stiffness of geogrid vertical settlement decreases up to an extent beyond this effect of stiffness reduces. Also, the optimum size of the aperture of geogrid is 1.4 × (Nominal Size of Ballast) being used.

Lal et al. (2016) conducted a review of rail-wheel contact stresses using software Ansys15.0 and Creo-parametric 2.0. For the modelling of rail International Union of Railways, guidelines were followed and, Indian guidelines for weight per unit length were obeyed. Results from the whole analysis showed that design is safe, and all stresses were with permissible range.

Esmaeili et al. (2018) investigated the consequences of geogrid reinforcement on bearing strength and vertical deformation of high railway embankment. In this research, both physical and numerical model were made and results were compared. Physical models were made to actual scale for different embankment heights (5m, 10m, 15m, 20m), for each height 5 models were made one without reinforcement and other four with the different number of the reinforcement layer. Numerical modelling was done using software PLAXIS and models similar to physical ones were simulated. Results revealed that an optimum number of reinforced layers for different embankment height were different beyond which further increase in reinforcement layer does improve the soil. Also, the effect of the tensile strength of geogrid reduces with the decrease in embankment height and by improving soil characteristics.

After literature review, following research gaps are observed –

1) The study on the confinement width of geocell is meagre.
2) Comparison of 2-D and 3-D models on railway geotechnics is less.
3) Effect of fineness of mesh generated for finite element model is underestimated.

To fulfil the observed research gap, an attempt has been made to work in this direction. Keeping the objectives in mind the study on numerical modelling on railway geotechnics on various aspects are presented in the following chapters.

CHAPTER 3

MATERIALS AND METHODS

As discussed in the objective for the analyses of subgrade stress, both 2-D and 3-D model of the rail track system were designed and simulations were carried out using fine element software Abaqus/CAE.

Abaqus/CAE is, finite element software firstly launched in 1978, used to create simulation models of various real-world problems like strength and toughness analysis of electronics or machine components, stress distribution in building structure or soil etc.

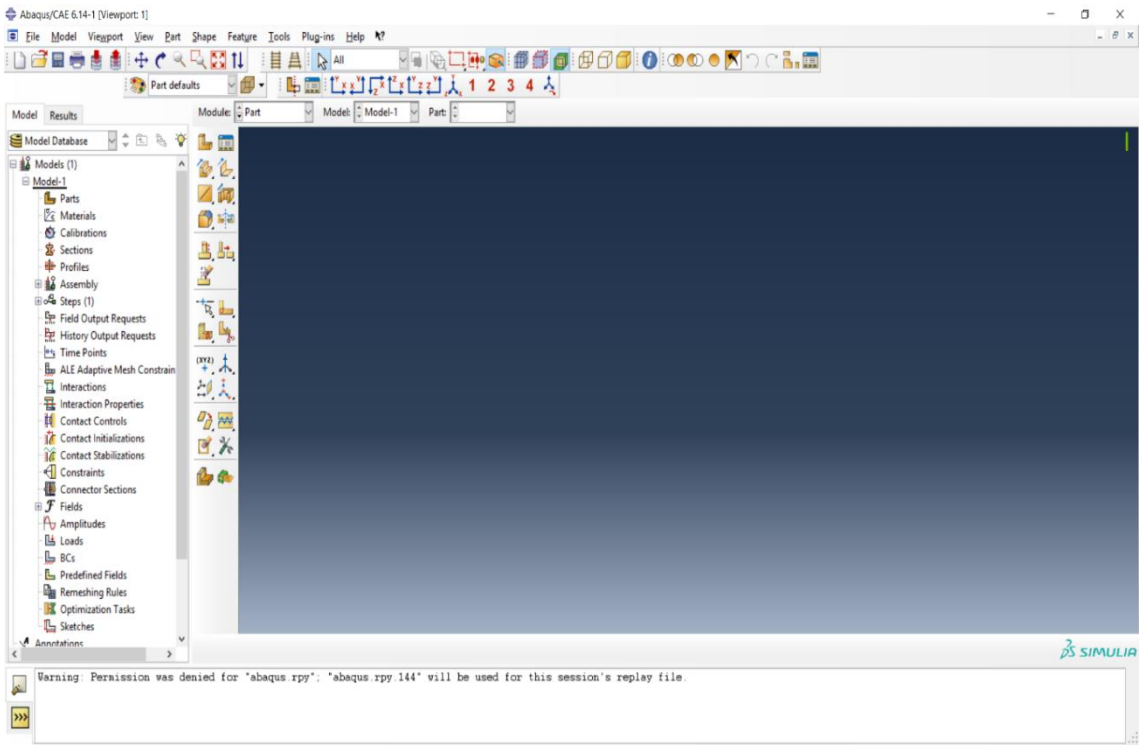

Figure 3.1 Basic Layout of Abaqus/CAE

Version of Abaqus/CAE used for conducting whole simulation and stress analyses of the subgrade is 6.14-1.

In the whole analysis, eight models were simulated including unreinforced and geocell confined ballast in 2-D analyses and same in case of 3-D analyses.

3.1 FE RAILWAY SUBSTRUCTURE GEOMETRY

All the models were designed in Abaqus/CAE and are in accordance with Indian Railway standards. Rail section considered for analysis is 52kg/m and its cross-section is shown in Figure 3.2 and dimensions are mentioned in Table 3.1

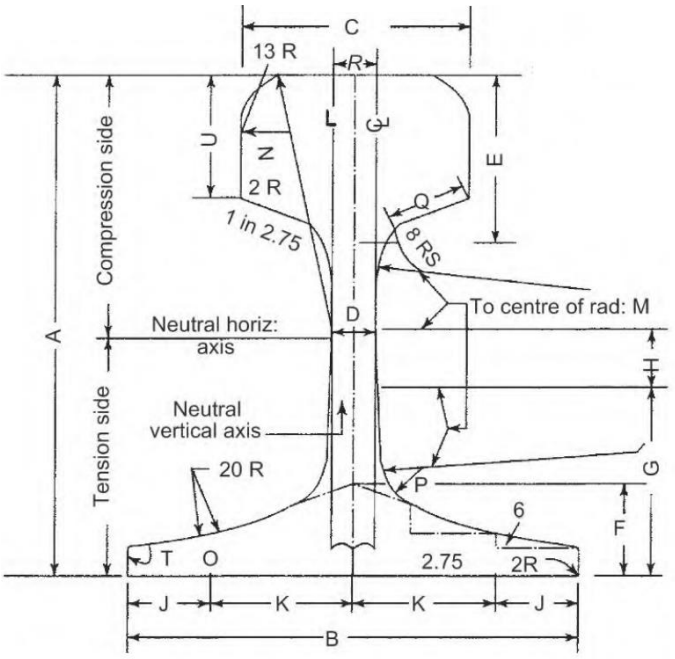

Figure 3.2 I.R.S 52kg/m Rail Section – Key To Dimension Table (Mundrey 2005)

Table 3.1 Dimension Table (Mundrey 2005)

Rail Section 52kg	Weight per metre	A	B	C	D	E	F	G	H	J	K
	Kg	mm	mm	mm	mm	mm	mm	mm	mm	mm	mm
	51.89	156	136	67	15.5	51	29	60	19	24	44
Rail Section 52kg	Weight per metre	L	M	N	O	P	Q	R	S	T	U
	Kg	mm	mm	mm	mm	mm	mm	mm	mm	mm	mm
	51.89	305	381	80	13	13	17.5	18	22.5	5	38.82

For modelling, sleeper considered was PCS-12 which made of prestressed concrete and sleeper density was taken as M+5

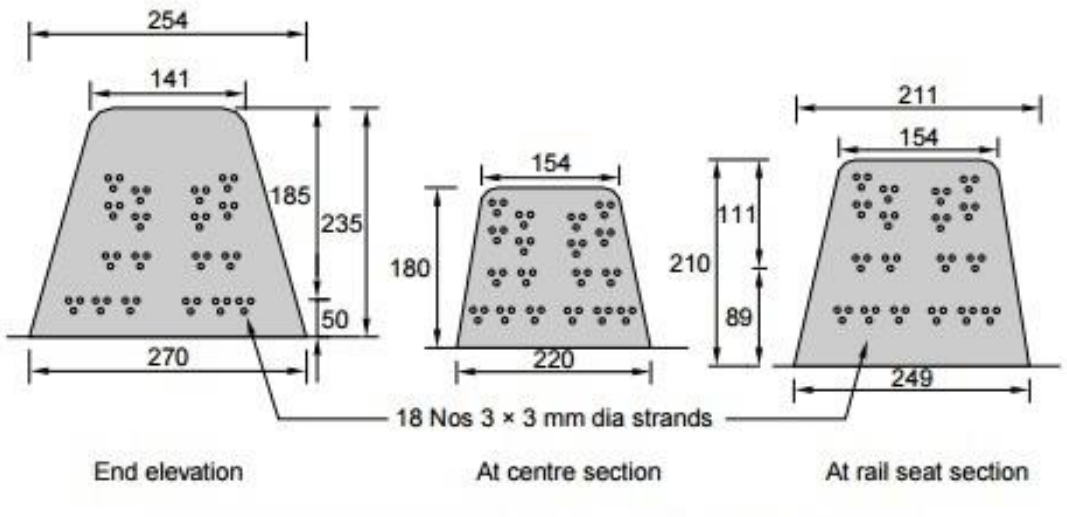

Figure 3.3 Cross Section of PCS-12 Sleeper (Agarwal 2017)

Width of ballast at base level is 4.6 m, and at the crest, the level is 3.4 m with a side slope of 1.5:1. 350 mm of the ballast layer was provided. In the case of reinforced ballast, geocell confinement was done at the centre of the ballast layer. Height of Geocell is 0.1 m, and its width varies from 1.88 m to 3.8 m. Width and depth of soil subgrade consider for the model is 7.10 m and 4.0 m respectively. Geometrical representation of 2-D Model analysed are shown in Figure 3.4 to Figure 3.11 where Figure 3.4 is a geometrical representation of the 2-D model with unreinforced ballast and rest figures are a geometrical representation of the 2-D model with different geocell confinement width.

Figure 3.4 Geometrical representation of 2-D Model with Unreinforced Ballast

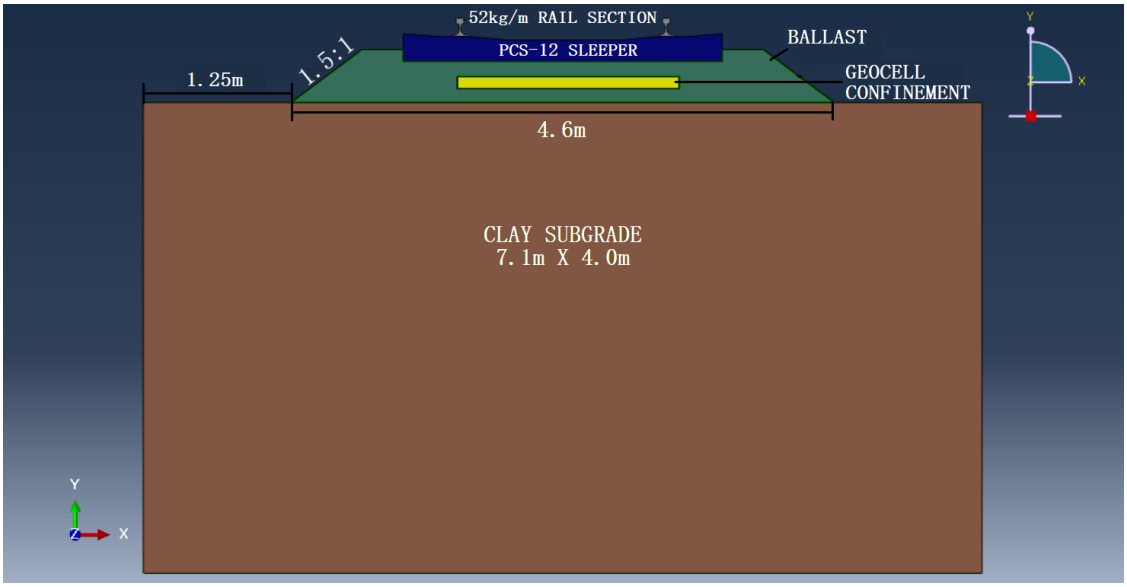

Figure 3.5 Geometrical representation of 2-D Model with Geocell Confinement Width 1.88m

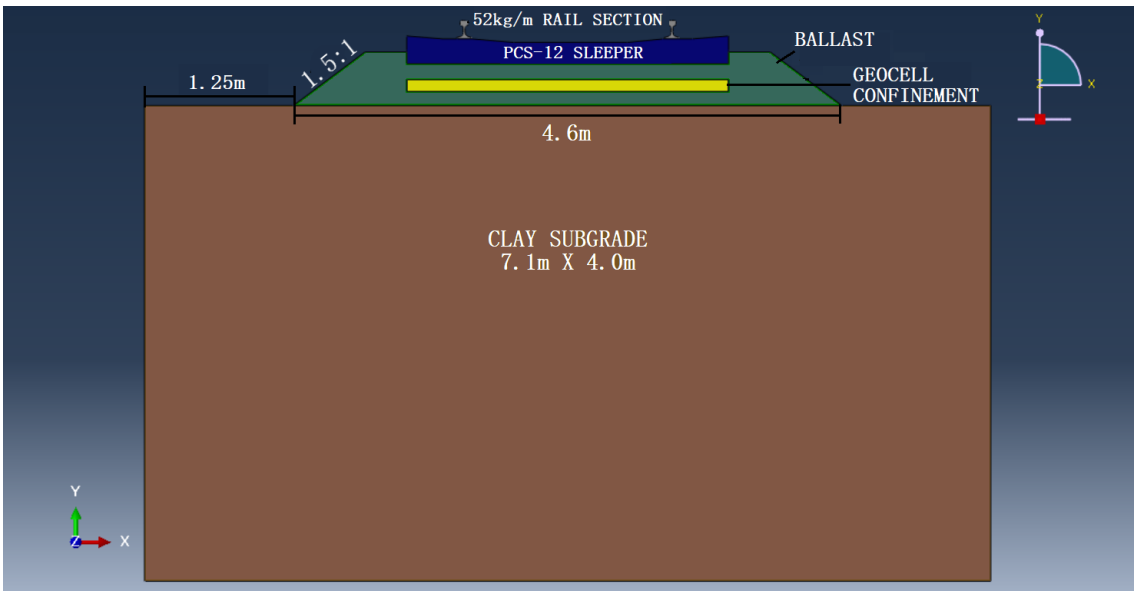

Figure 3.6 Geometrical representation of 2-D Model with Geocell Confinement Width 2.7m

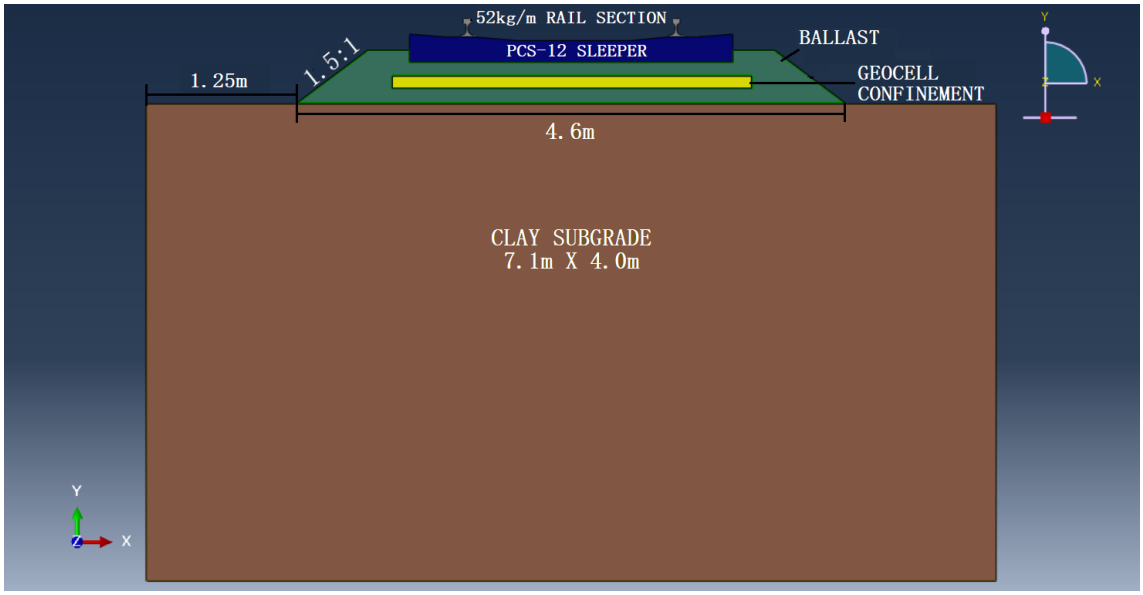

Figure 3.7 Geometrical representation of 2-D Model with Geocell Confinement Width 3.0m

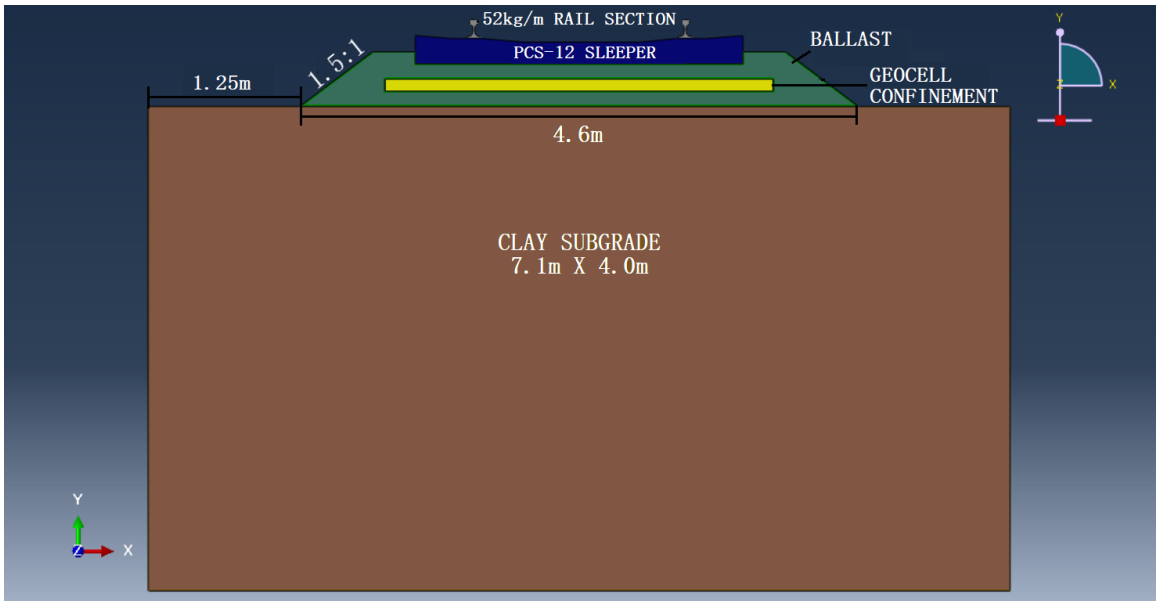

Figure 3.8 Geometrical representation of 2-D Model with Geocell Confinement Width 3.2m

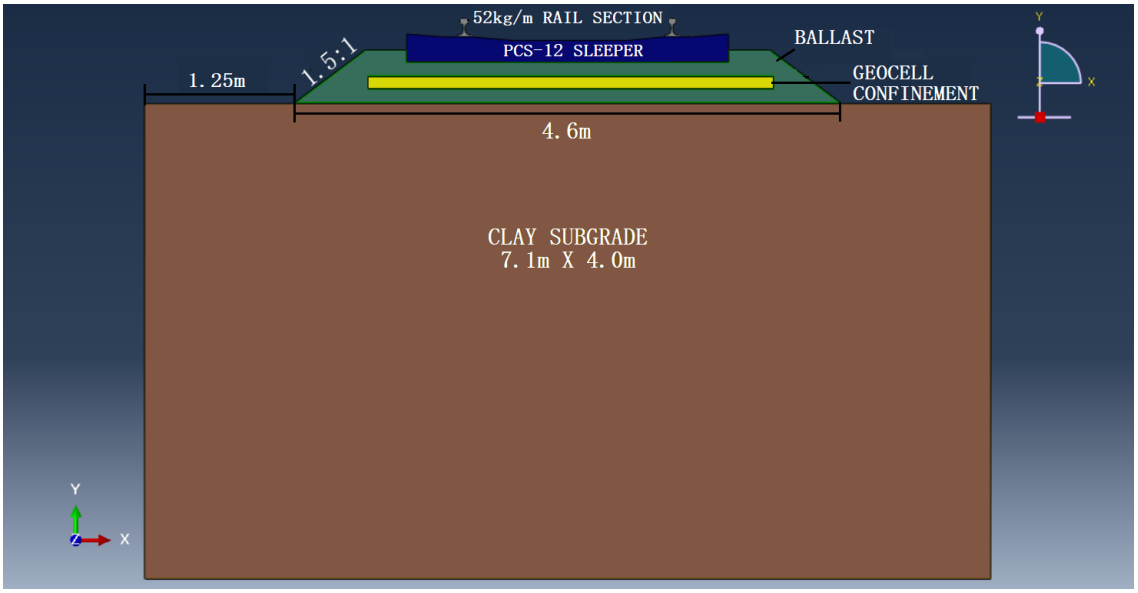

Figure 3.9 Geometrical representation of 2-D Model with Geocell Confinement Width 3.4m

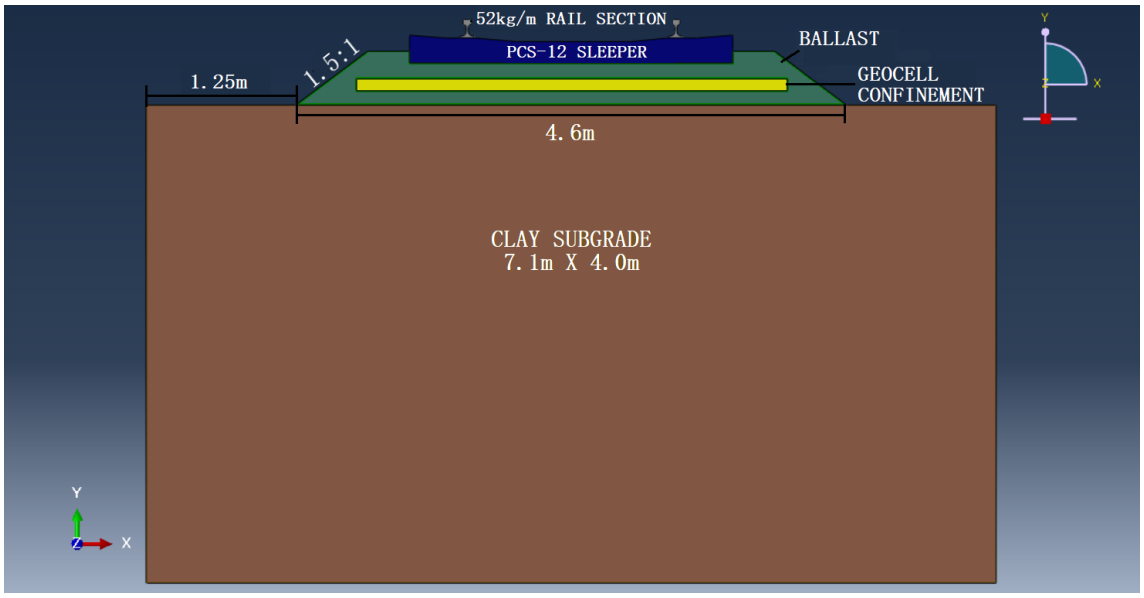

Figure 3.10 Geometrical representation of 2-D Model with Geocell Confinement Width 3.6m

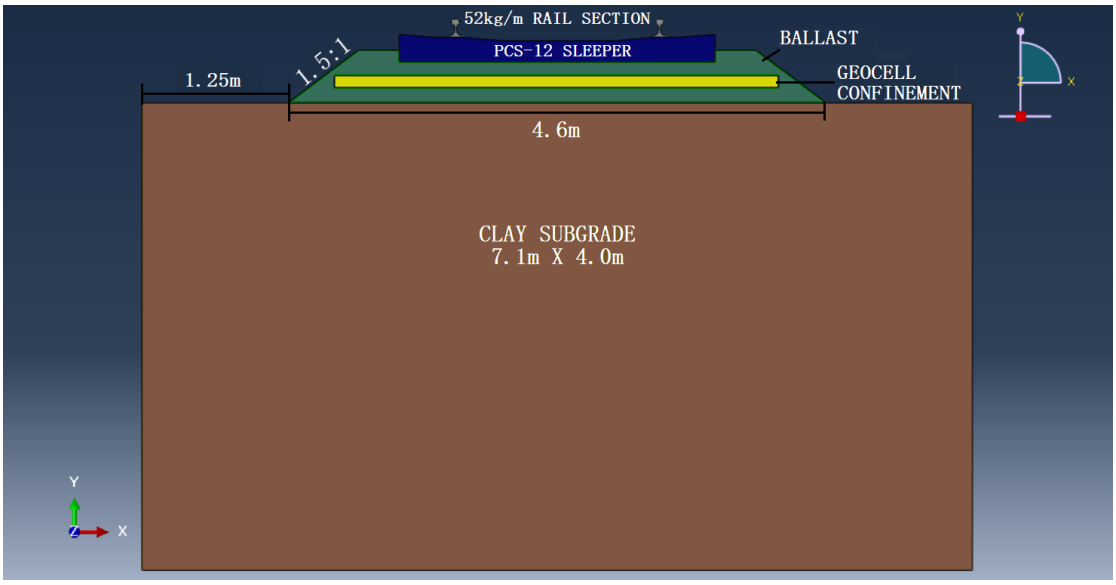

Figure 3.11 Geometrical representation of 2-D Model with Geocell Confinement Width 3.8m

In the case of 3-D analyses, all models were designed in a similar manner as in the case of 2-D analyses and extrusion of 4.692m is given. Geometrical representation of 3-D models is shown in Figure 3.12 to Figure 3.19.

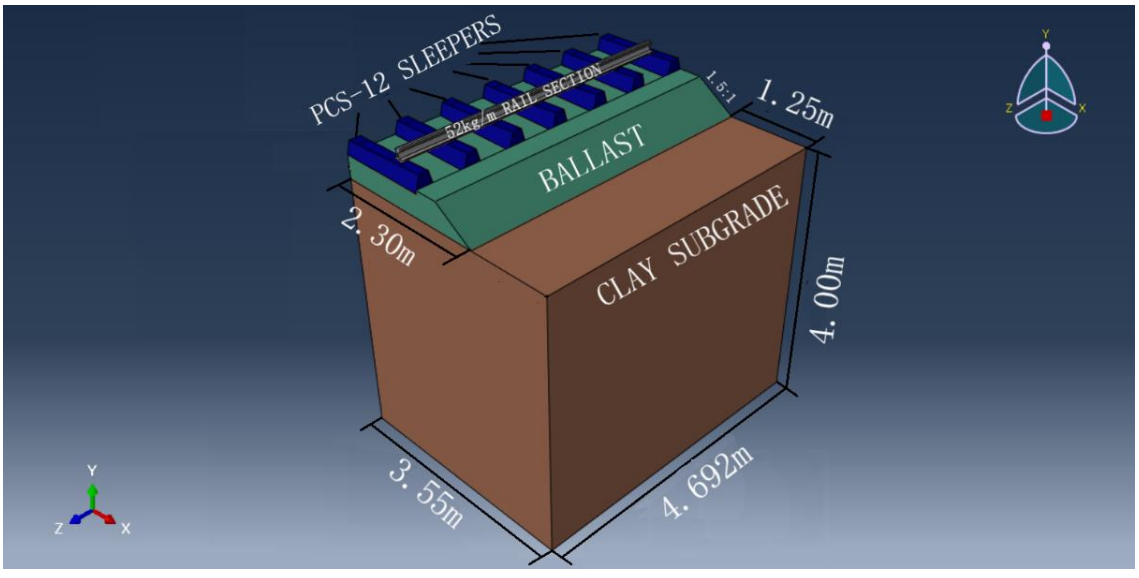

Figure 3.12 Geometrical representation of Axi-symmetric 3-D Model with Unreinforced Ballast

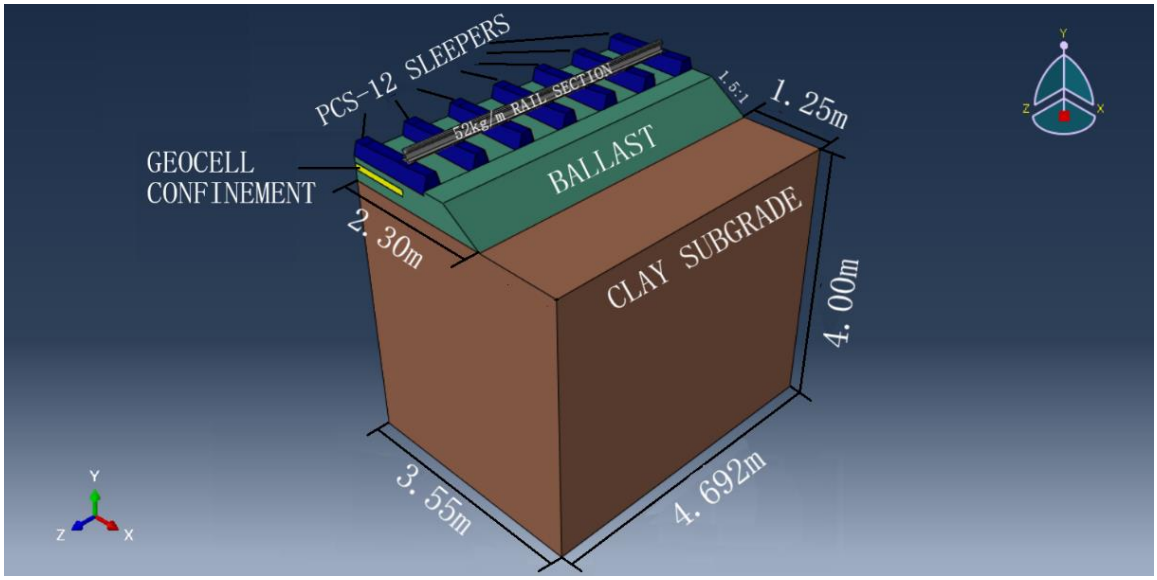

Figure 3.13 Geometrical representation of Axi-symmetric 3-D Model with Geocell Confinement Width 1.88m

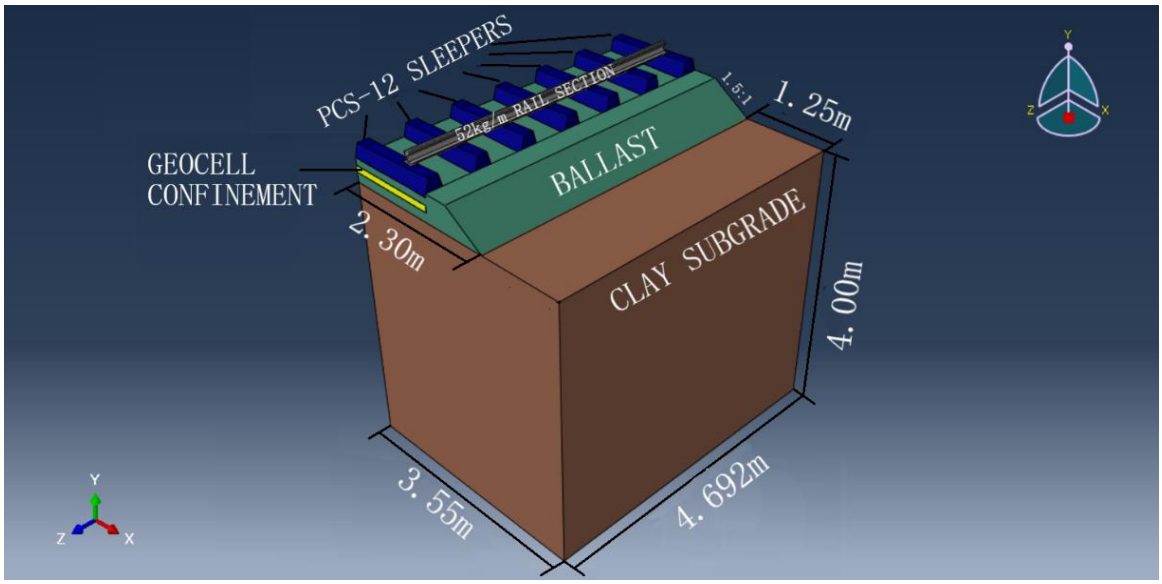

Figure 3.14 Geometrical representation of Axi-symmetric 3-D Model with Geocell Confinement Width 2.7m

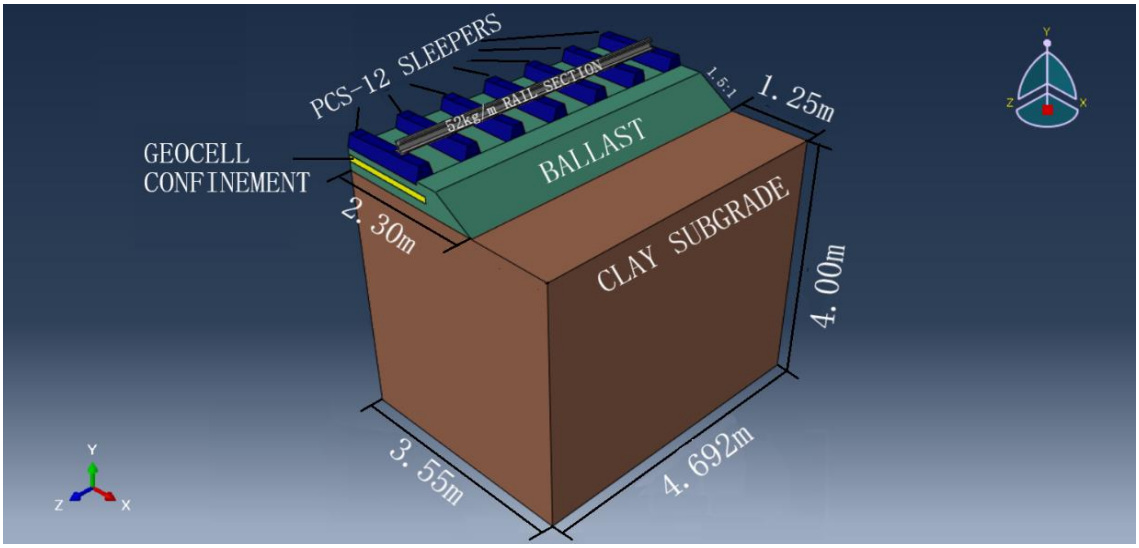

Figure 3.15 Geometrical representation of Axi-symmetric 3-D Model with Geocell Confinement Width 3.0m

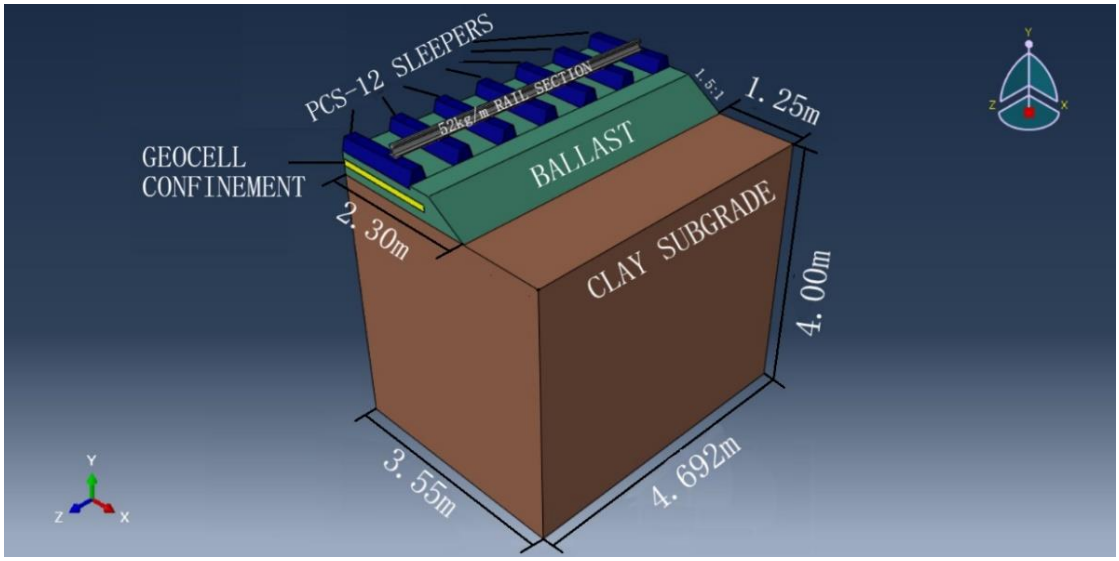

Figure 3.16 Geometrical representation of Axi-symmetric 3-D Model with Geocell Confinement Width 3.2m

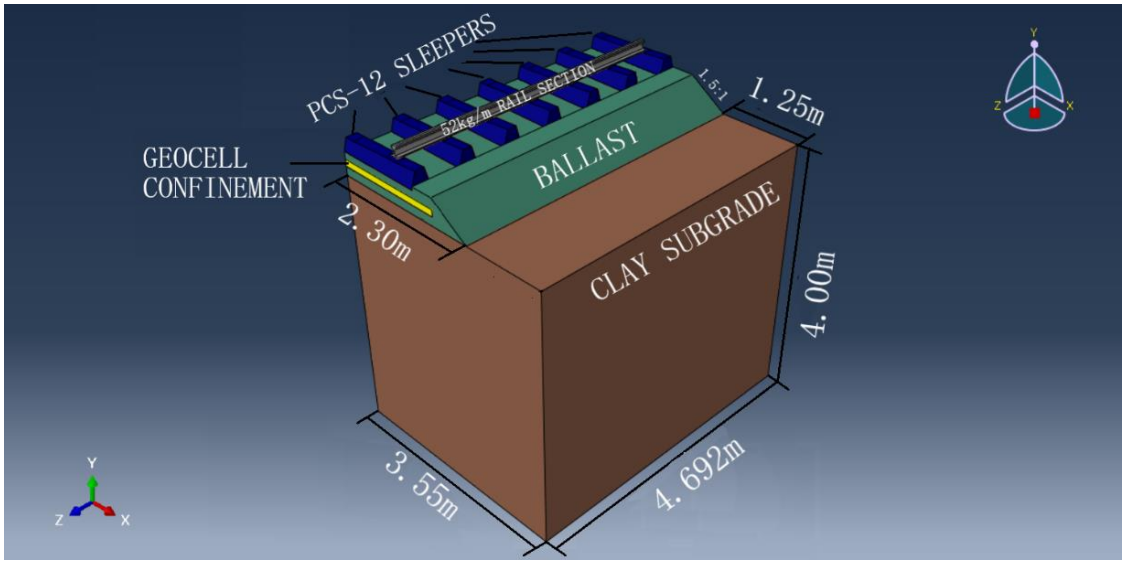

Figure 3.17 Geometrical representation of Axi-symmetric 3-D Model with Geocell Confinement Width 3.4m

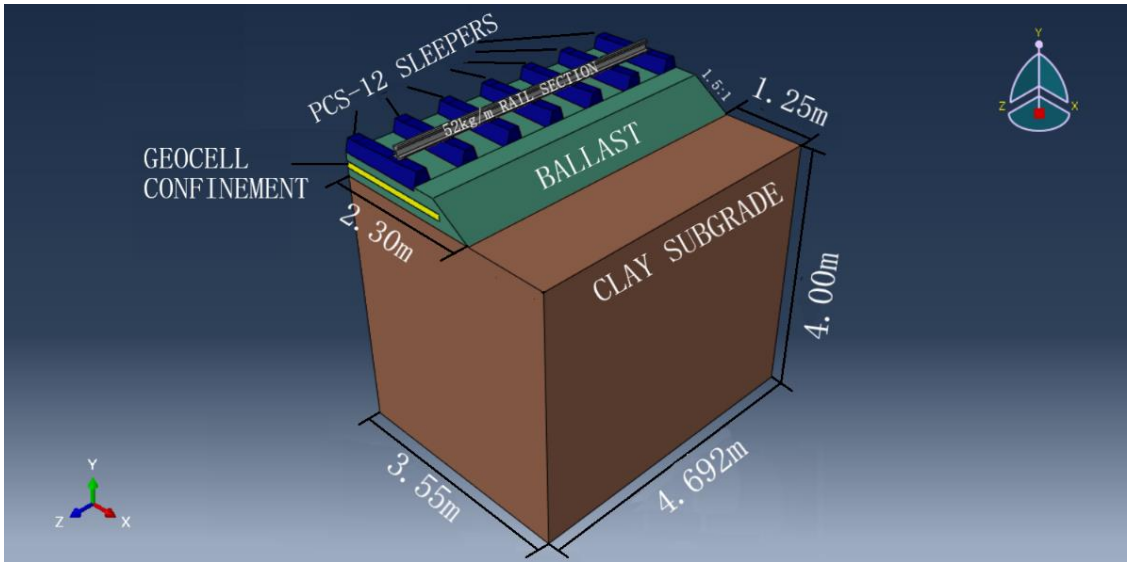

Figure 3.18 Geometrical representation of Axi-symmetric 3-D Model with Geocell Confinement Width 3.6m

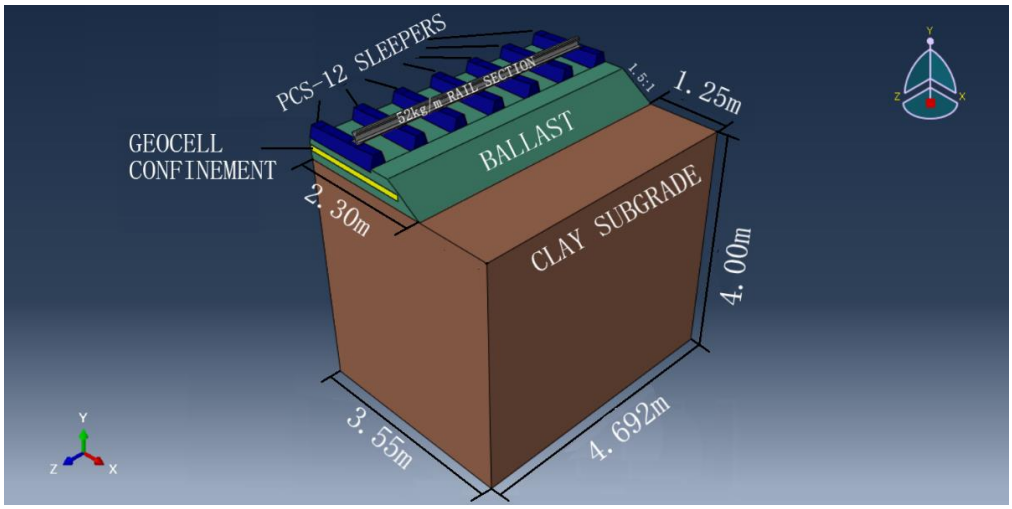

Figure 3.19 Geometrical representation of Axi-symmetric 3-D Model with Geocell Confinement Width 3.8m

3.2 FE MATERIAL PROPERTIES

For modelling, subgrade was taken as soft clay and low strength aggregate was taken as ballast. The rail and sleepers were taken in accordance with Indian Rail Standard. Geocell considered in all models was made of Novel Polymeric Alloy (NPA) rather than standard material because it had greater stiffness and creep resistance in comparison to standard materials like polyethene (Leshchinsky et al. 2013). During analysis rail, sleepers, geocell and subgrade had been simulated as an elastic material. While ballast and sub-ballast had been simulated as elasto-plastic material where plastic properties were given in accordance to Mohr-Coulomb Criterion with very little cohesion of $1kPa$ (Leshchinsky et al. 2013), for enabling of the simulation process. Subgrade was considered as elastic in order to decrease the computational cost. Material properties used for defining different component of numerical models are given in Table 3.2 and Table 3.3.

Table 3.2 FE Material Properties (Leshchinsky et al. 2013; Lal et al. 2016; Kumar and Sambasivarao 2014)

MATERIAL	Mass Density ρ (kg/m^3)	Elastic Modulus E(MPa)	Poisson's Ratio μ	Internal Angle of Friction φ (°)	Angle of Dilation ψ(°)
Rail	7850	200000	0.267	-	-
Sleeper	2400	30000	0.300	-	-
Ballast	1520	2	0.350	45	15
GeoCell	1500	2070	0.350	-	-

Table 3.3 FE Subgrade Properties

MATERIAL	Mass Density ρ (kg/m^3)	Elastic Modulus E(MPa)	Poisson's Ratio μ	Internal Angle of Friction φ (°)	Angle of Dilation ψ(°)
Clay Subgrade	1600	2	0.15	-	-

3.3 FE MESH AND BOUNDARY CONDITIONS

Meshing is a procedure of dividing a part of the finite element model into small fragments. Mesh can be triangular, rectangular and square in shape. For finite element analysis, the meshing of parts is required, as shown in Figure 3.20 and Figure 3.21 in the case of the 2-D model. Figure 3.20 shows a meshed model with unreinforced ballast and Figure 3.21 gives a representation of the meshed model with geocell confined ballast. In the 2-D model, the Element type of ballast mesh was CPE6M. CPE6M has been selected for the interlocking effect of granular ballast materials (Leshchinsky et al. 2013). For sleepers and clay element type CPE8R. For rail and geocell element type CPE4R for meshing was used. All part except the clay subgrade (coarsely modelled) was modelled finely. Interaction between different parts was taken in such a way that there was no sliding. The whole model was a constraint in the x-direction to prevent lateral displacement. Also, the base of clay subgrade was a constraint in the whole direction.

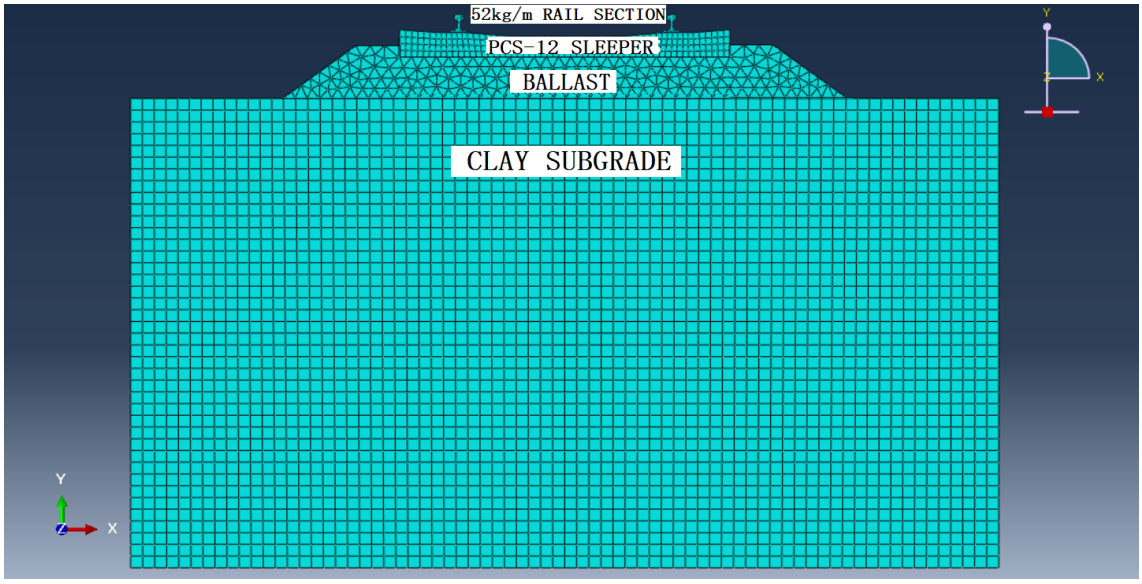

Figure 3.20 2-D Meshed Model with Unreinforced Ballast

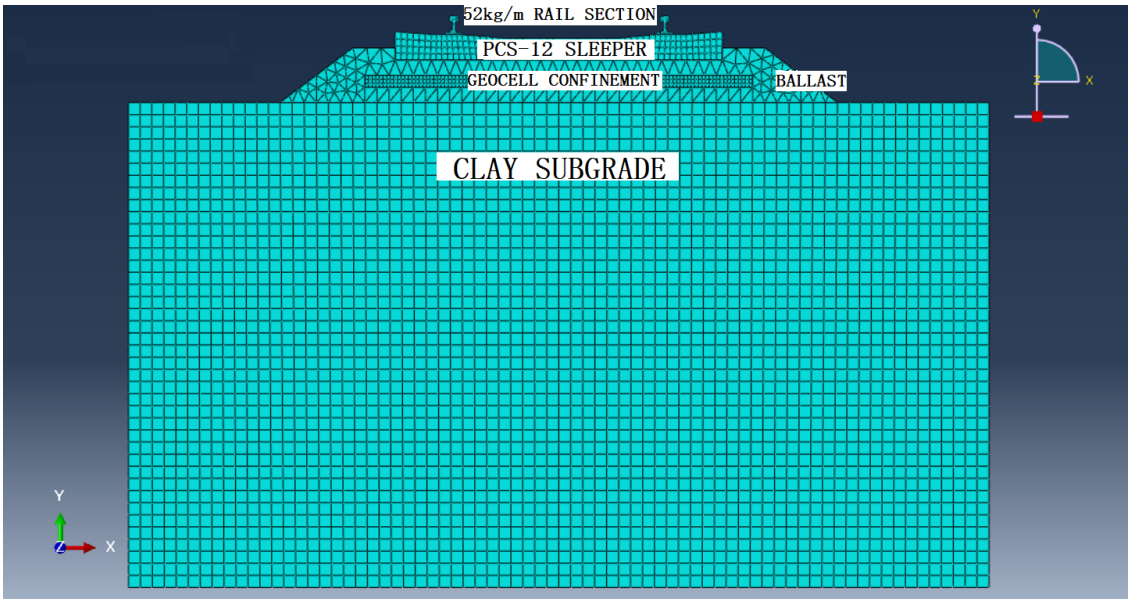

Figure 3.21 2-D Meshed Model with Geocell Confined Ballast

In the 3-D model, the Element type of ballast mesh was C3D10I. C3D10I had been selected for the interlocking effect of granular ballast materials (Leshchinsky et al. 2013). For sleepers, geocell and clay element type C3D8R.For rail element type C3D4, for meshing is used. All part except the clay subgrade (coarsely modelled) was modelled finely. Interaction between different parts was taken in such a way that there was no sliding. The whole 3-D model was constraint in x-direction as well as z-direction. Also the base of clay subgrade was constraint in whole direction i.e encastre. Figure 3.22 shows the meshed model with unreinforced ballast and Figure 3.23 gives a representation of the meshed model with geocell confined ballast.

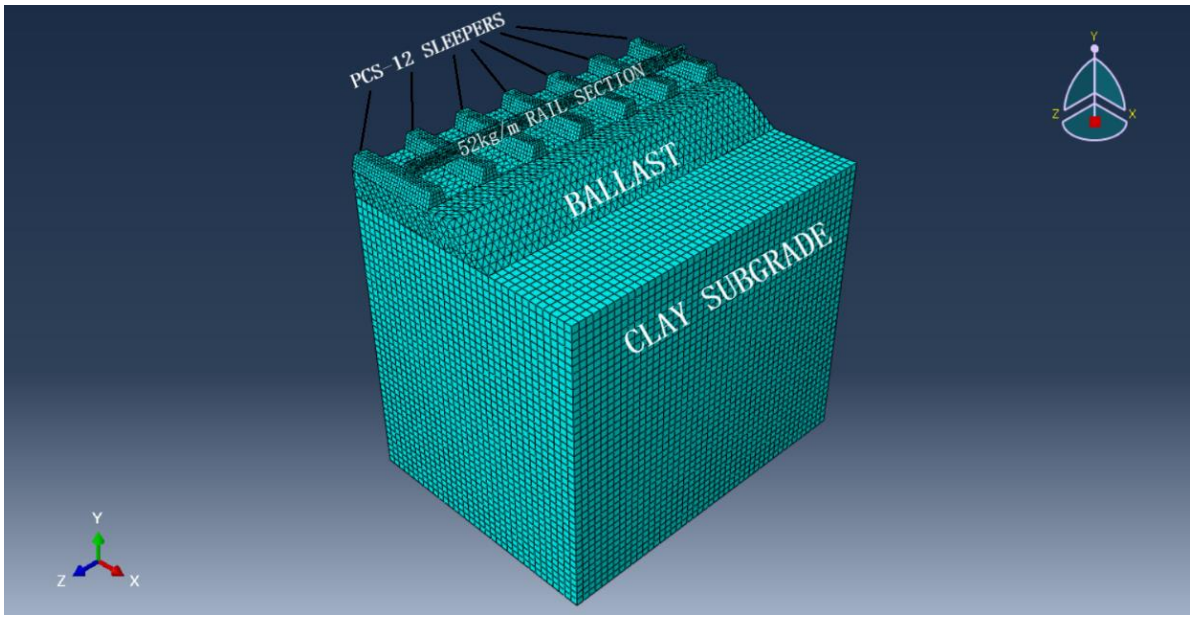

Figure 3.22 Axi-symmetric 3-D Meshed Model with Unreinforced Ballast

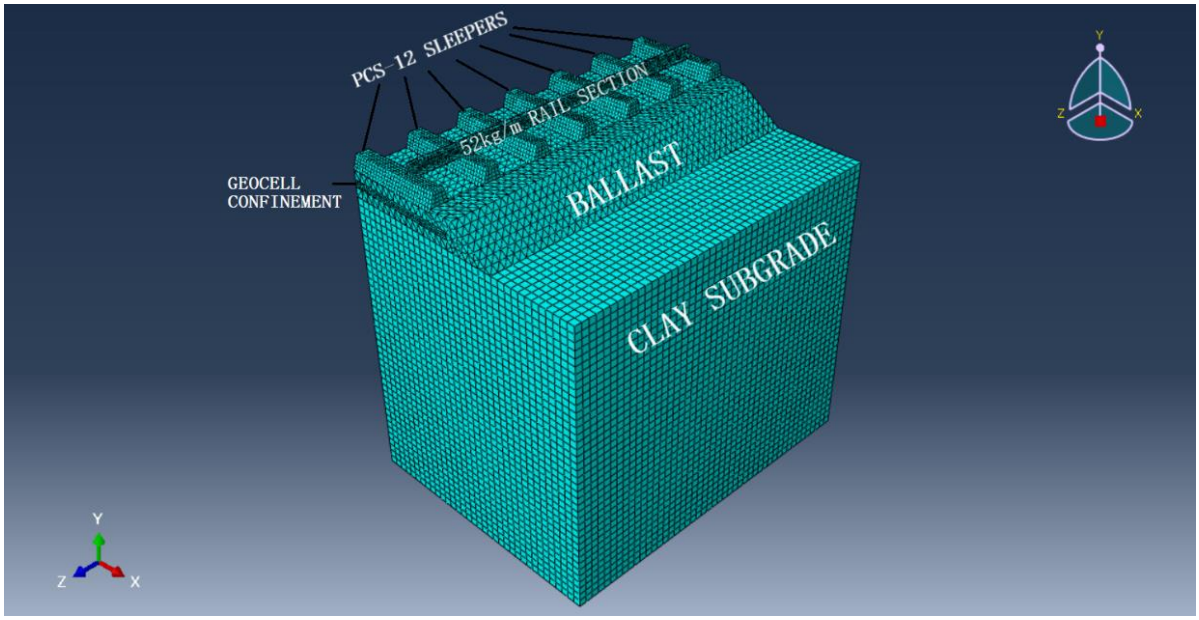

Figure 3.23 Axi-symmetric 3-D Meshed Model with Geocell Confined Ballast

3.4 FE MESH CONVERGENCE AND MODEL VALIDATION

Meshing is the essence of finite element analysis. Compatibility of whole FE model depends upon element type and size of the mesh. Mesh convergence is the procedure in which it is verified that any change size of mesh does not result in drastic changes in the results. For this purpose, a model was analysed for different mesh properties as given in

Table 3.4 and plot between the entity to analysed and relative mesh density was plotted, shown in Figure 3.24

Table 3.4 Mesh Information

Mesh Size (m)	No. of Elements	Relative Mesh Density (%)
0.30	4292	2.30
0.25	6940	3.72
0.20	12617	6.77
0.15	30090	16.15
0.14	36376	19.52
0.13	46203	24.79
0.12	55812	29.95
0.11	74021	39.72
0.10	94698	50.81
0.09	129781	69.64
0.08	186370	100

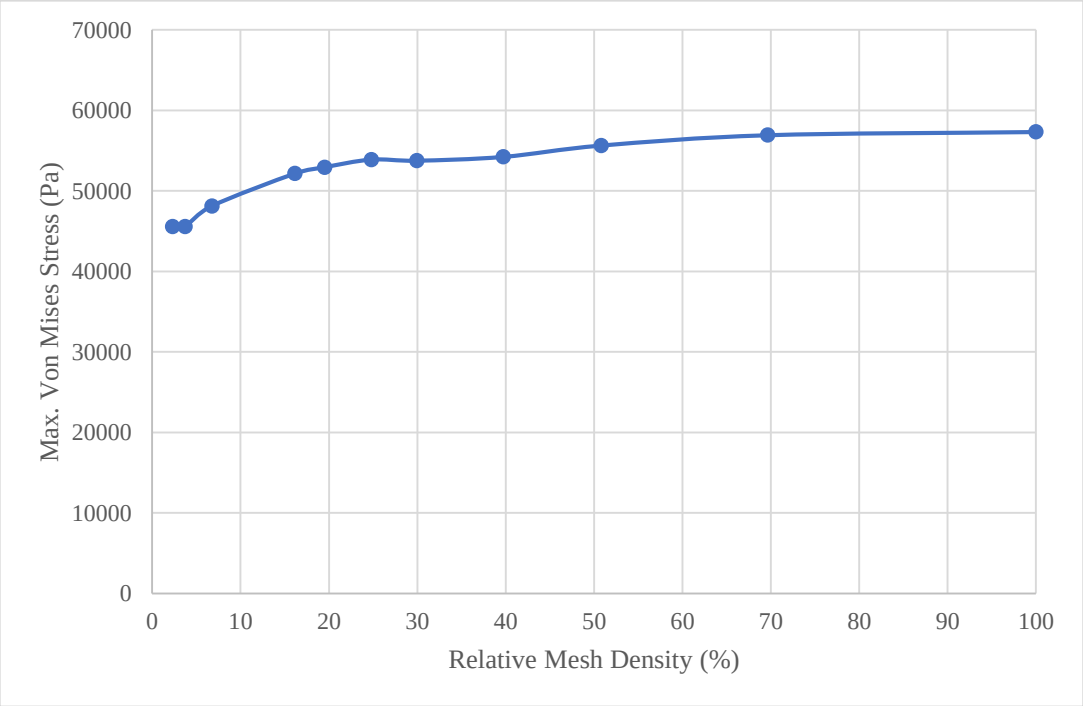

Figure 3.24 Graphical representation of Mesh Convergence

From Table 3.4 and Figure 3.24, there was very minimal change in the result of analysis in models having mesh finer than 0.1m. But there was one more factor that plays a role in mesh size selection which computational cost which affects the economics of the whole

project. Figure 3.25 is a plot between CPU time required to complete the whole analysis and relative mesh density.

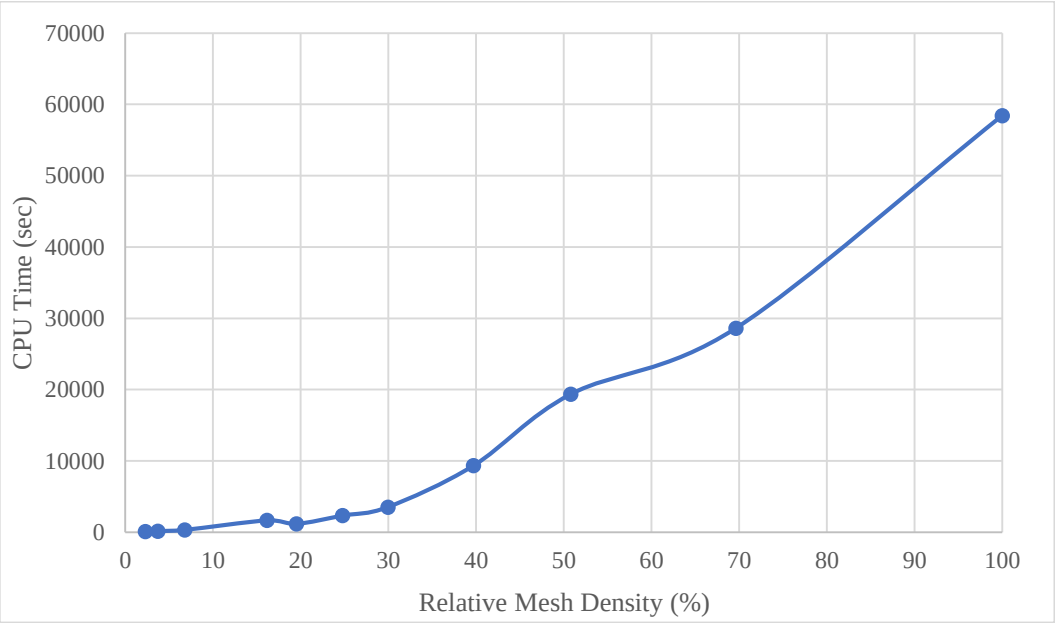

Figure 3.25 Graph between CPU Time and Relative Mesh Density

From both Figure 3.24 and 3.25, mesh size of 0.1 m was selected for all analyses throughout the project as it is economics in comparison to the finer meshes and give better results in comparison to coarser meshes.

For the validation of analysis, a particular of amount of load was applied on a portion of model shown in Figure 3.26 instead of the whole model and stresses were determined.

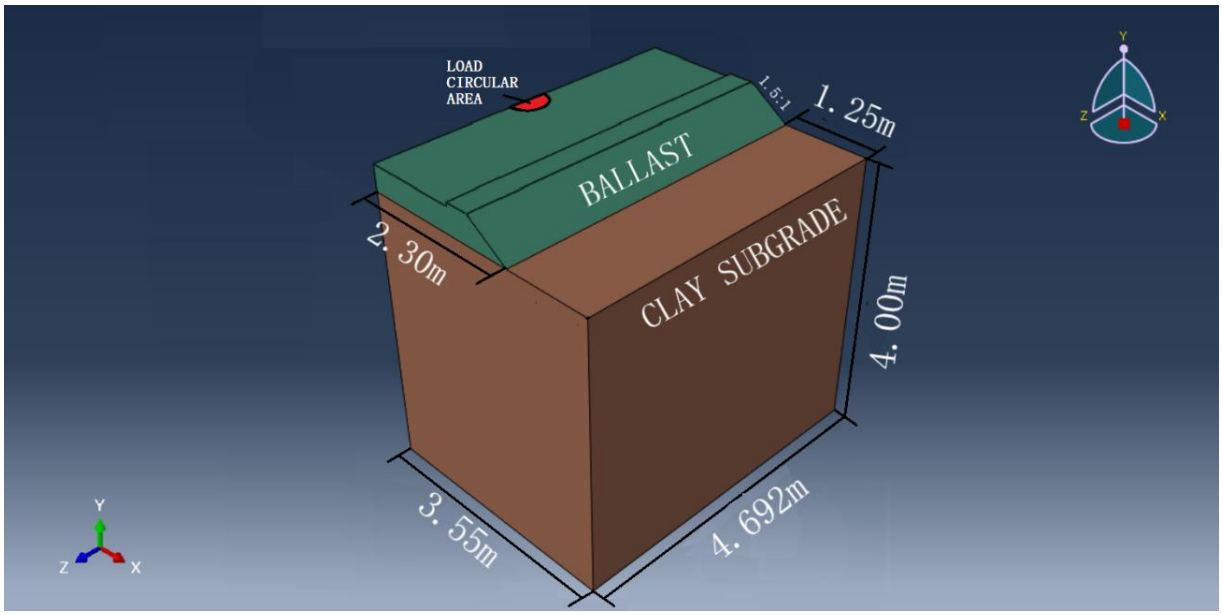

Figure 3.26 Geometrical representation of Axi-symmetric 3-D Model for validation

Also, the same problem is solved using Boussinesq's solution for the circularly loaded area.

$$\sigma_y = q \times \left[1 - \frac{y^3}{(b^2+y^2)^{3/2}}\right] \tag{3.1}$$

where,

σ_y – Vertical Stresses at depth ' y ' (Pa)

q – Load applied per unit area (Pa)

b – Radius of circular loaded area (m)

y – Depth at which stress are to be calculated (m)

In validation model,

$$q = 100000\ Pa$$

$$b = 0.3m$$

$$y = 0.35m$$

Using Equation (3.1),

$$\sigma_y = 100000 \times \left[1 - \frac{0.35^3}{(0.3^2 + 0.35^2)^{3/2}}\right]$$

$$\sigma_y = 56231\ Pa$$

In Table 3.5, results for the validation model are given.

Table 3.5 Variation of Maximum Vertical Stress with mesh size

Mesh Size (m)	Vertical Stress (Pa) at depth 0.35m
0.30	45574.6
0.25	45563.8
0.20	48113.4
0.15	52144.5
0.14	52936.1
0.13	53888.4
0.12	53752.0
0.11	54221.3
0.10	55632.9
0.09	56919.6
0.08	57316.5

It can be observed that value of selected mesh 0.1m gives vertical stresses equal to 55632.9 Pa while 0.09m mesh size gives better result but the difference between the computational cost justifies the selection of 0.1m mesh size.

3.5 FE LOADING

The wheel load for the broad gauge is limited to 11.25 tonnes (Mundrey 2005). As train moves instead of static, condition becomes quasi-static. To account the effect of train speed, speed factor (SF) was introduced (Mundrey 2005) and its value was determined from Figure 3.27.

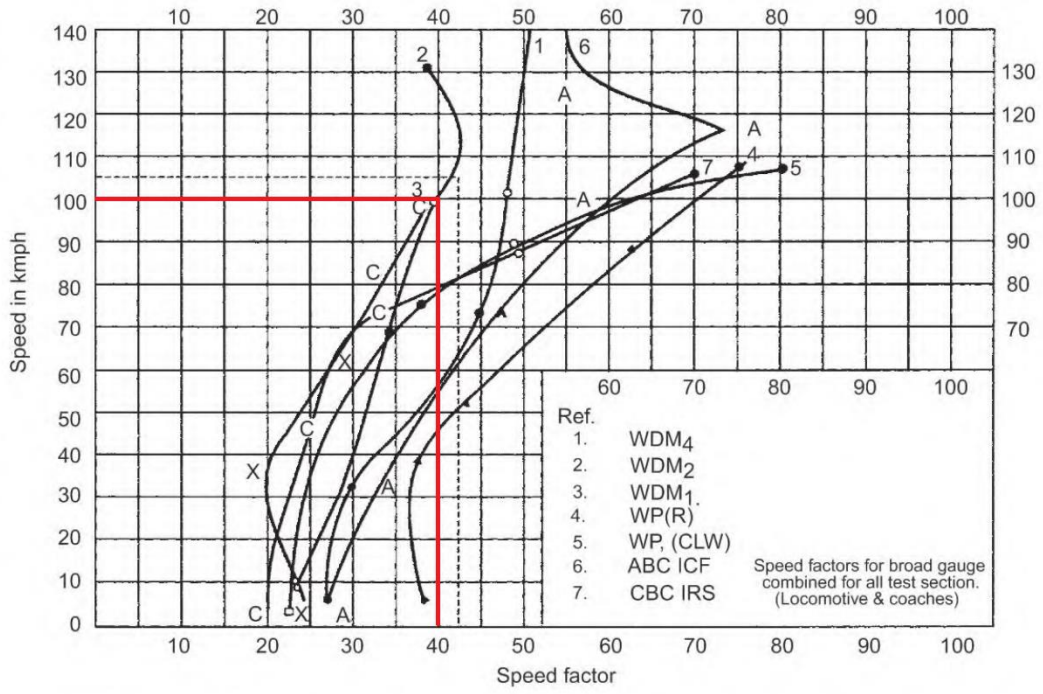

Figure 3.27 Speed vs Speed Factor Chart (Mundrey 2005)

Also to account the dynamic effect of rail load while analysing the models, dynamic factor was considered as following:-

$$P_d = \varphi P_s \qquad \text{(Van Dyk et al. 2015)} \qquad (3.2)$$

where P_d – Dynamic Wheel Load

P_s – Static Wheel Load

Φ – Dynamic Wheel Load Factor

$$\varphi = 1 + \frac{v}{3\times\sqrt{U}} \qquad \text{(Srinivasan 1969)} \qquad (3.3)$$

where Φ – Dynamic Wheel Load Factor

V – Speed of Train (mile/h)

U – Track Modulus (psi)

To take the rail load considered on the conservative side, both above-mentioned factors were considered.

$$P = SF \times \varphi \times P_S \quad (3.4)$$

Where P – Factored Load

SF – Speed Factor

Φ – Dynamic Wheel Load Factor

Assuming, v $= 100\ km/h = 62.13\ mile/h$

U = $6000\ psi$ (Van Dyk et al. 2015)

$P_s = 11.25\ tonnes$

From Equation (3.3), $\varphi = 1 + \frac{62.13}{3\times\sqrt{6000}}$

$\varphi = 1.267$

From Figure 3.25 $S.F = 1.4$

From Equation (3.4), $P = 1.4 \times 1.267 \times 11.25$

$P \approx 20\ tonnes \approx 200kN$

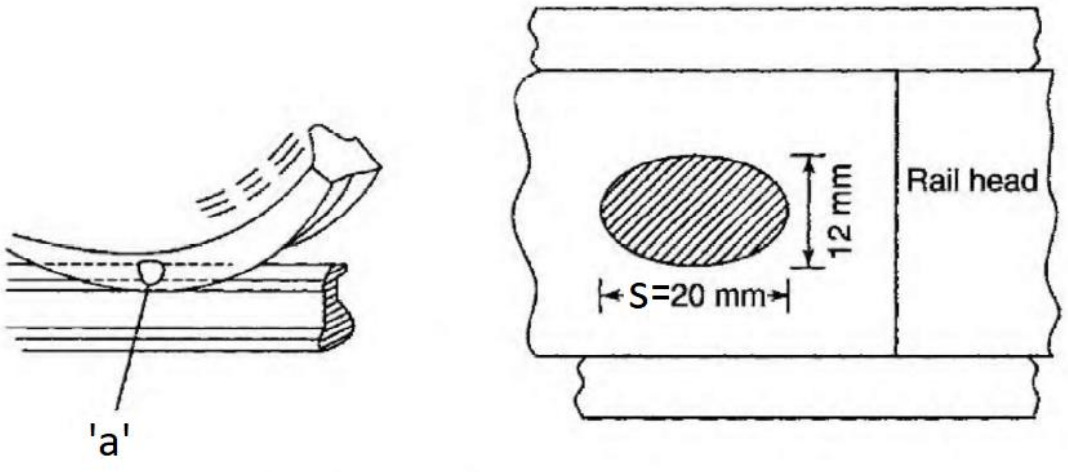

Figure 3.28 Contact area between Wheel and Rail Track (Mundrey 2005)

Contact Area (a) = $1.88 \times 10^{-4}\ m^2$ (as shown in Figure 3.28)

Contact Pressure due to Rail Load = $\frac{P}{a}$ (3.5)

$$= \frac{200000}{1.88\times10^{-4}}$$

$$= 1.063 \times 10^{9} kN/m^2$$

For determining the duration of load application: -

$$v = r\omega \quad (3.6)$$

$$\theta = \frac{s}{r} \quad (3.7)$$

$$\omega = \frac{\theta}{t} \quad (3.8)$$

where,

r – radius of wheel (m) = 0.420m

ω – angular velocity of the wheel (sec^{-1})

v – velocity of the wheel (m/sec)

θ – central angle subtended by 's' length

s – length of contact between wheel and rail track

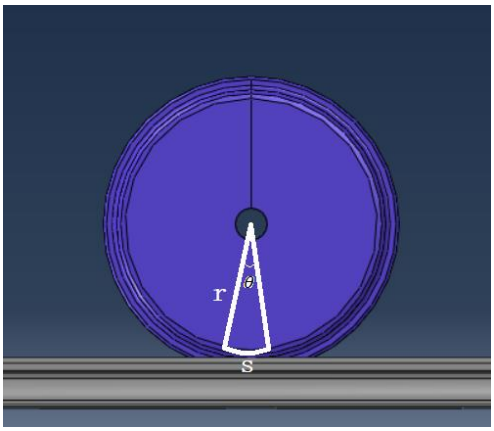

Figure 3.29 Contact between Wheel and Rail Track

With the reference of Figure 3.29 following calculation were done:

From Equation (3.6),

$$\frac{100 \times 5}{18} = .42 \times \omega$$

$$\omega = 66.13\ sec^{-1}$$

From Equation (3.7),

$$\theta = \frac{0.020}{0.420}$$

$$\theta = 0.0463\ radians$$

From Equation (3.8),

$$66.13 = \frac{0.0463}{t}$$

$$t = 7 \times 10^{-4} sec$$

Therefore in all 3-D FE models, the contact pressure of $1.063 \times 10^{9} kN/m^{2}$ was applied over an area of $1.88 \times 10^{-4} m^{2}$ for a time period of $7 \times 10^{-4} sec$. Also in all 2-D models, the contact pressure of $1.08 \times 10^{7} kN/m^{2}$ for a time period of $7 \times 10^{-4} sec$.

3.6 FE PROBLEM SIZE

1) 2-D Model Problem (Unreinforced)
   - Number of Elements 3846
   - Number of Nodes 5602
   - Total Number of Variables in the Model 10822
2) 2-D Model Problem (Geocell Confinement Width - 1.88m)
   - Number of Elements 4146
   - Number of Nodes 6035
   - Total Number of Variables in the Model 11298
3) 2-D Model Problem (Geocell Confinement Width – 2.7m)
   - Number of Elements 4277
   - Number of Nodes 6225
   - Total Number of Variables in the Model 11510
4) 2-D Model Problem (Geocell Confinement Width – 3.0m)
   - Number of Elements 4328
   - Number of Nodes 6305

Total Number of Variables in the Model 11612

5) 2-D Model Problem (Geocell Confinement Width – 3.2m)

Number of Elements 4361

Number of Nodes 6353

Total Number of Variables in the Model 11668

6) 2-D Model Problem (Geocell Confinement Width – 3.4m)

Number of Elements 4389

Number of Nodes 6393

Total Number of Variables in the Model 11712

7) 2-D Model Problem (Geocell Confinement Width – 3.6m)

Number of Elements 4418

Number of Nodes 6429

Total Number of Variables in the Model 11744

8) 2-D Model Problem (Geocell Confinement Width – 3.8m)

Number of Elements 4455

Number of Nodes 6489

Total Number of Variables in the Model 11824

9) 3-D Model Problem (Unreinforced)

Number of Elements 109437

Number of Nodes 135390

Total Number of Variables in the Model 372098

10) 3-D Model Problem (Geocell Confinement Width - 1.88m)

Number of Elements 150630

Number of Nodes 210715

Total Number of Variables in the Model 518239

11) 3-D Model Problem (Geocell Confinement Width – 2.7m)

Number of Elements 167727

Number of Nodes 241708

Total Number of Variables in the Model 578038

12) 3-D Model Problem (Geocell Confinement Width – 3.0m)

Number of Elements 173836

Number of Nodes 253138

Total Number of Variables in the Model 599528

13) 3-D Model Problem (Geocell Confinement Width – 3.2m)

Number of Elements 177721

Number of Nodes 260191

Total Number of Variables in the Model 613271

14) 3-D Model Problem (Geocell Confinement Width – 3.4m)

Number of Elements 182579

Number of Nodes 268946

Total Number of Variables in the Model 630286

15) 3-D Model Problem (Geocell Confinement Width – 3.6m)

Number of Elements 186302

Number of Nodes 275738

Total Number of Variables in the Model 643312

16) 3-D Model Problem (Geocell Confinement Width – 3.8m)

Number of Elements 190282

Number of Nodes 282949

Total Number of Variables in the Model 657487

CHAPTER 4

RESULTS AND DISCUSSION

In total, sixteen simulations were run in Abaqus/CAE and stress in clay subgrade during each simulation was observed. On comparing the results of simulation in regarding stresses in both cases, unreinforced ballast and geocell confined ballast, improvement in stress distribution was observed. The reason behind the improvement was the inclusion of geocell confinement resulting in a wider distribution of stresses generally over its width. Also, it was observed that results of 3-D models were more reliable than 2-D models as in 2-D models, its parts behaved like beam instead of a slab. Thus stress distribution along the longitudinal direction was negligible. Figure 4.1 to Figure 4.8 gives subgrade stress distribution contours of 2-D models with unreinforced ballast and geocell confined ballast. For graphical comparison, as shown in Figure 4.9, a plot between subgrade stress at depth 0.1 m below the subgrade surface and length along with the ballast.

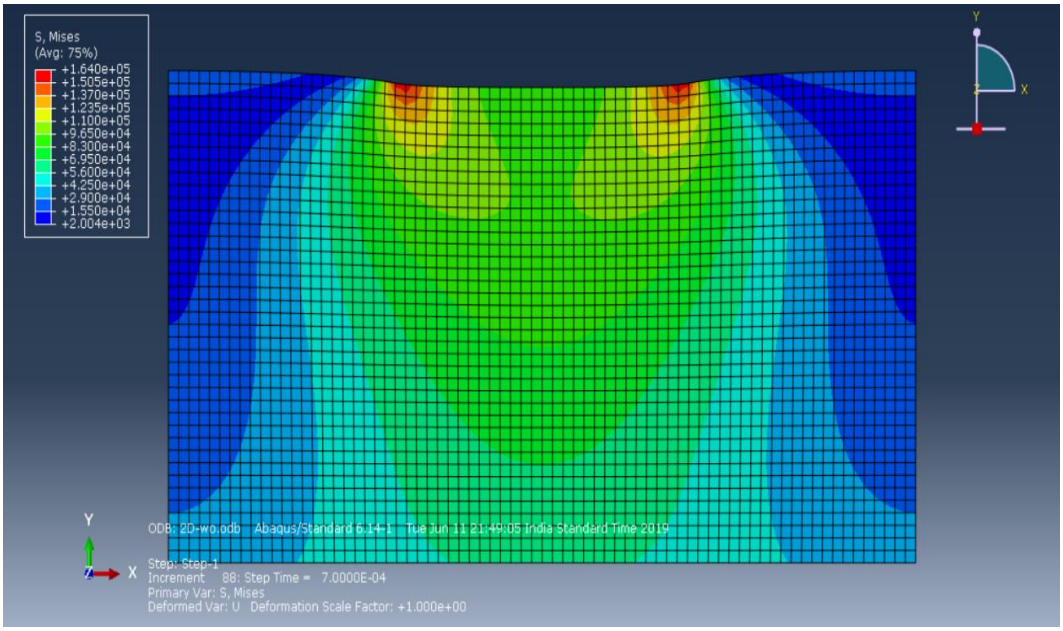

Figure 4.1 Subgrade Stress Distribution in 2-D Model with Unreinforced Ballast

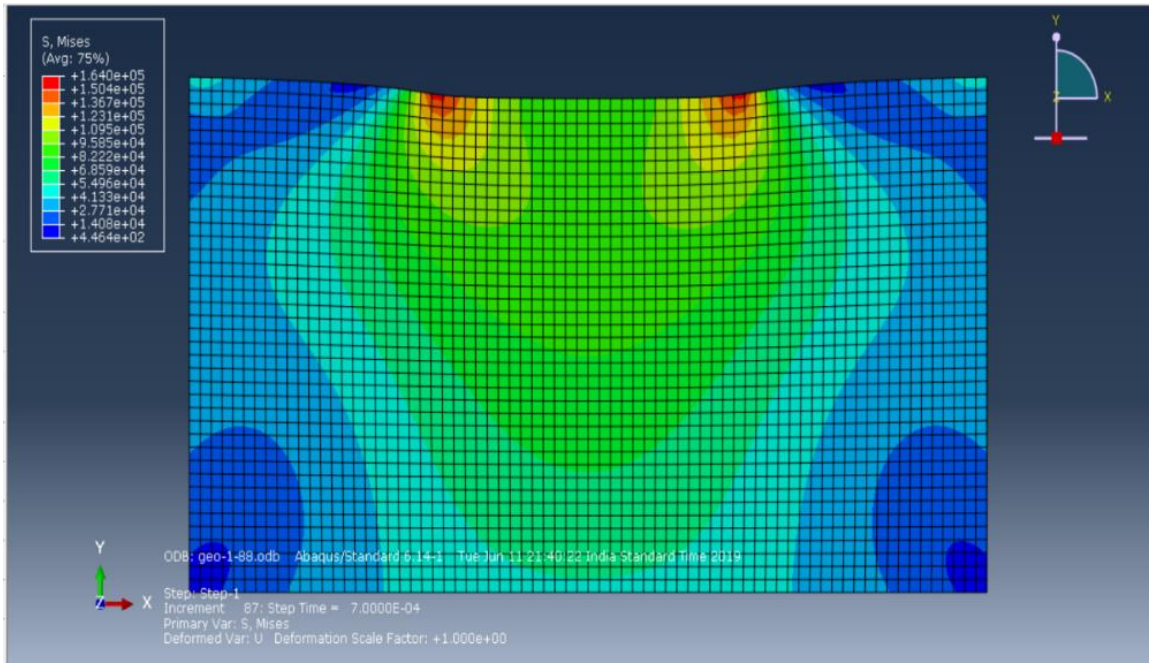

Figure 4.2 Subgrade Stress Distribution in 2-D Model with Geocell Confinement Width 1.88m

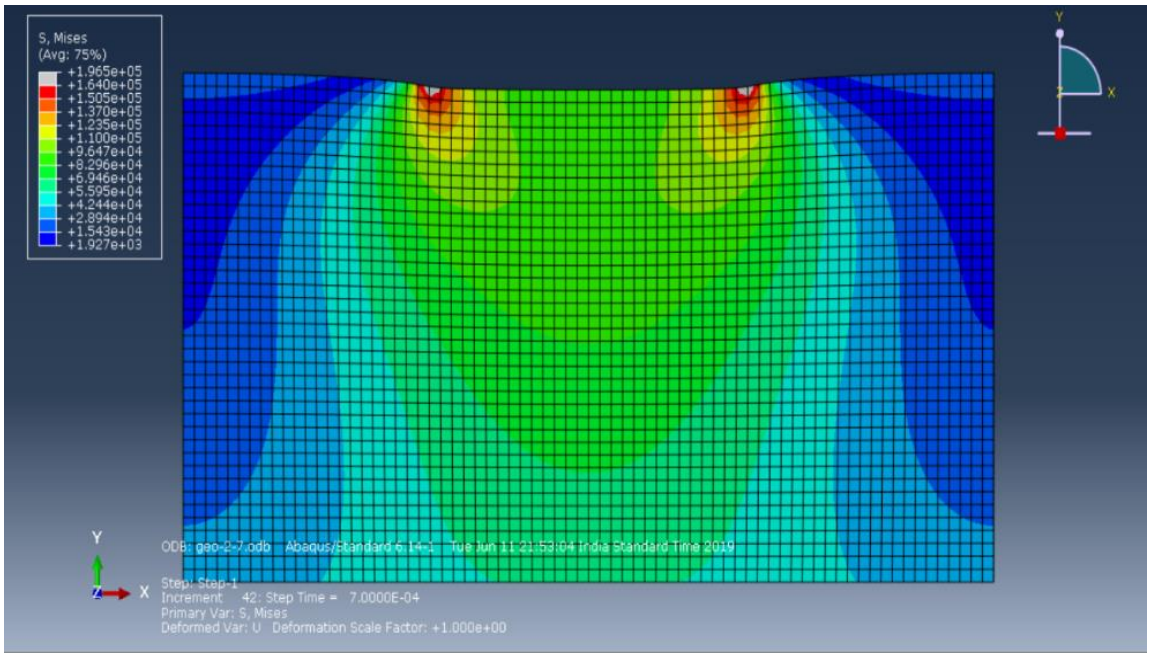

Figure 4.3 Subgrade Stress Distribution in 2-D Model with Geocell Confinement Width 2.7m

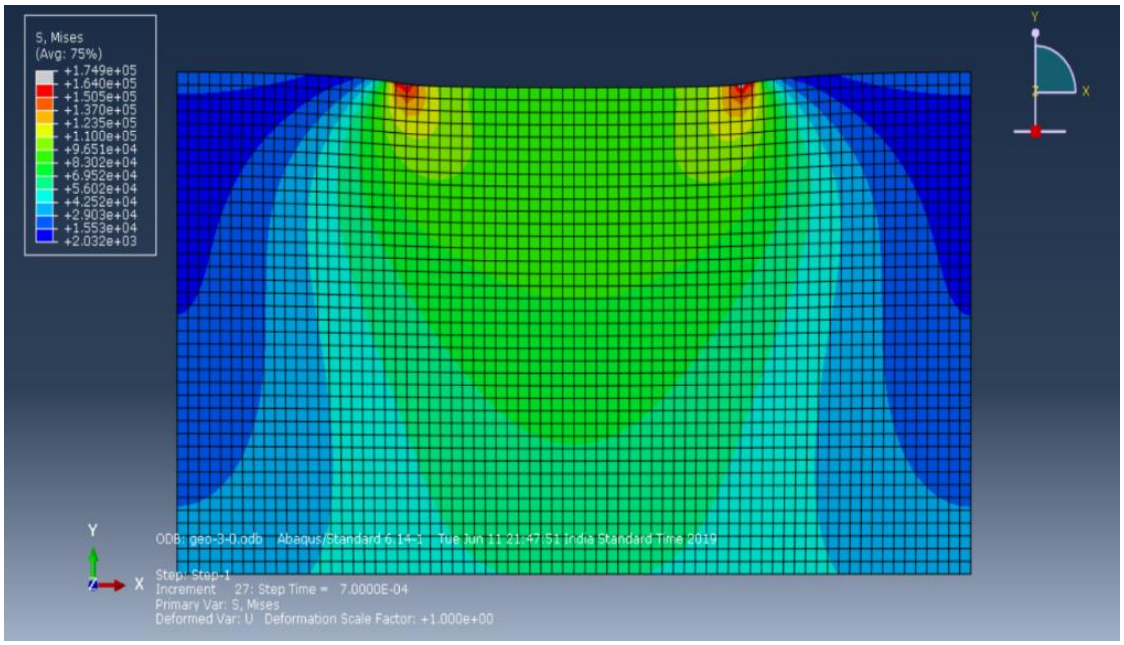

Figure 4.4 Subgrade Stress Distribution in 2-D Model with Geocell Confinement Width 3.0m

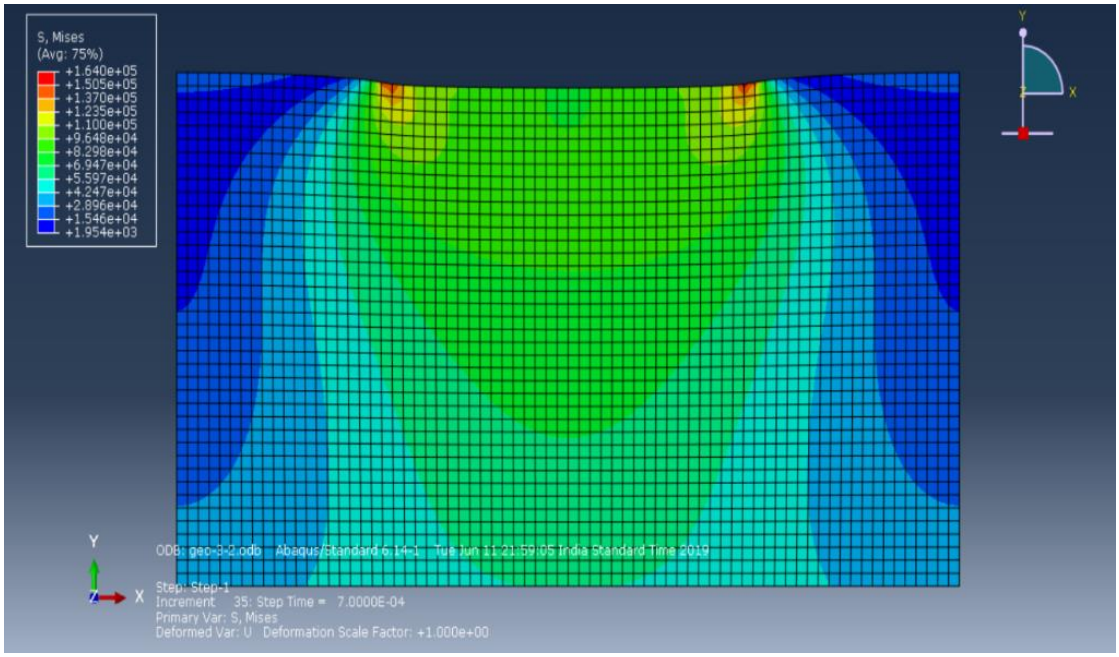

Figure 4.5 Subgrade Stress Distribution in 2-D Model with Geocell Confinement Width 3.2m

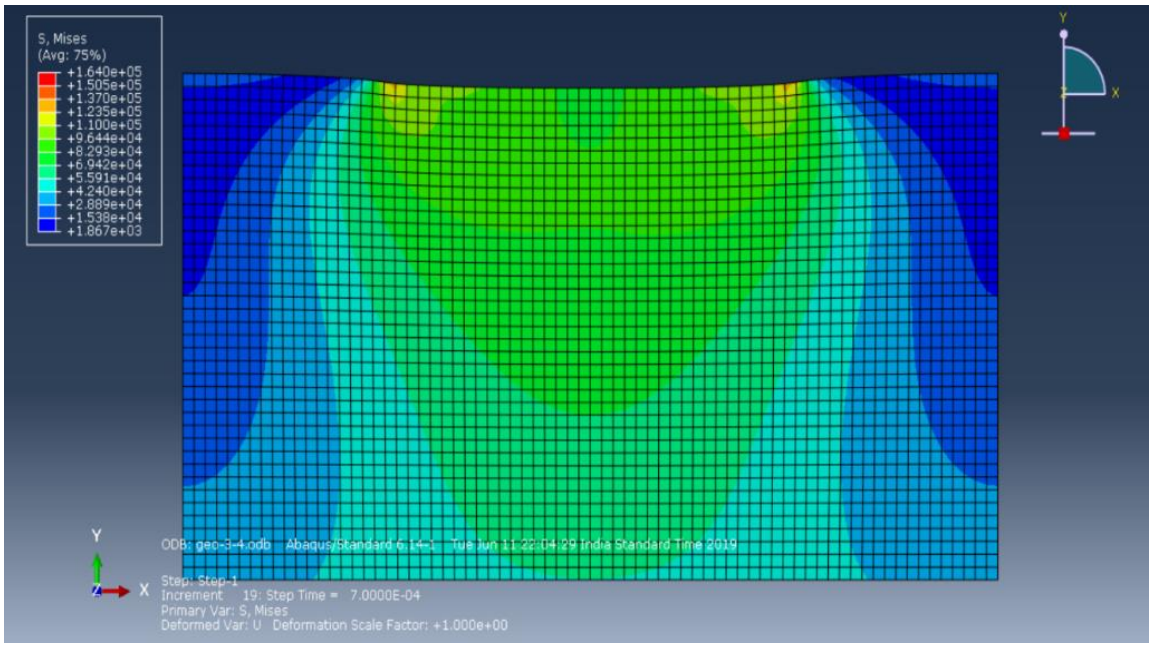

Figure 4.6 Subgrade Stress Distribution in 2-D Model with Geocell Confinement Width 3.4m

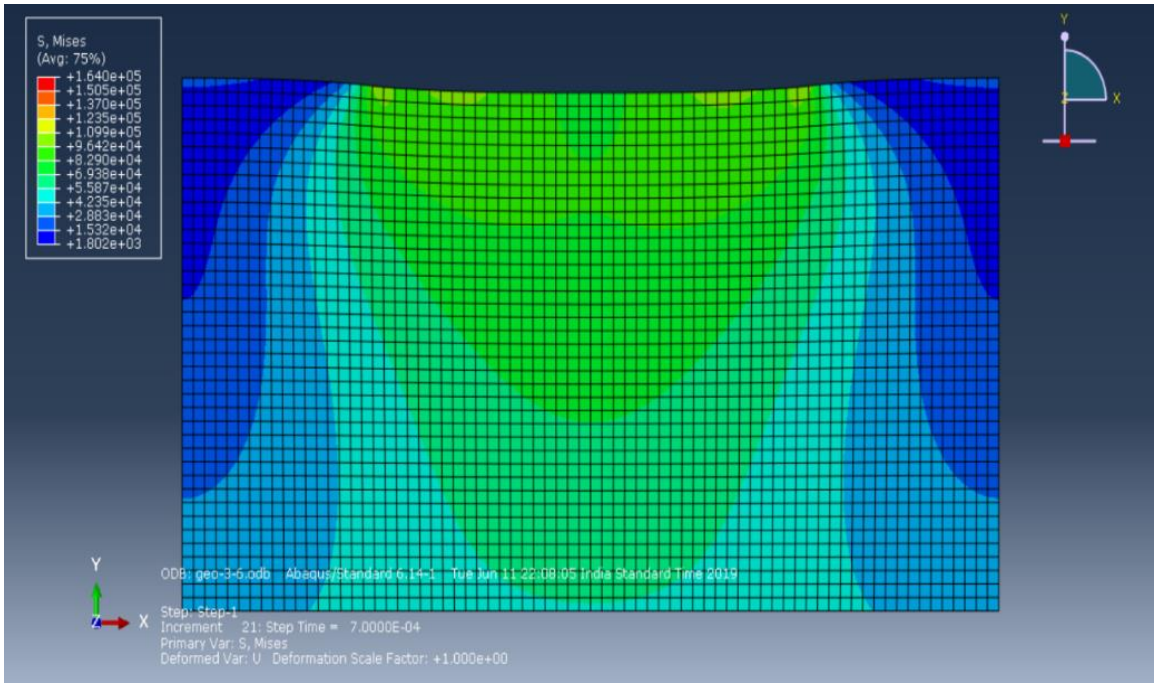

Figure 4.7 Subgrade Stress Distribution in 2-D Model with Geocell Confinement Width 3.6m

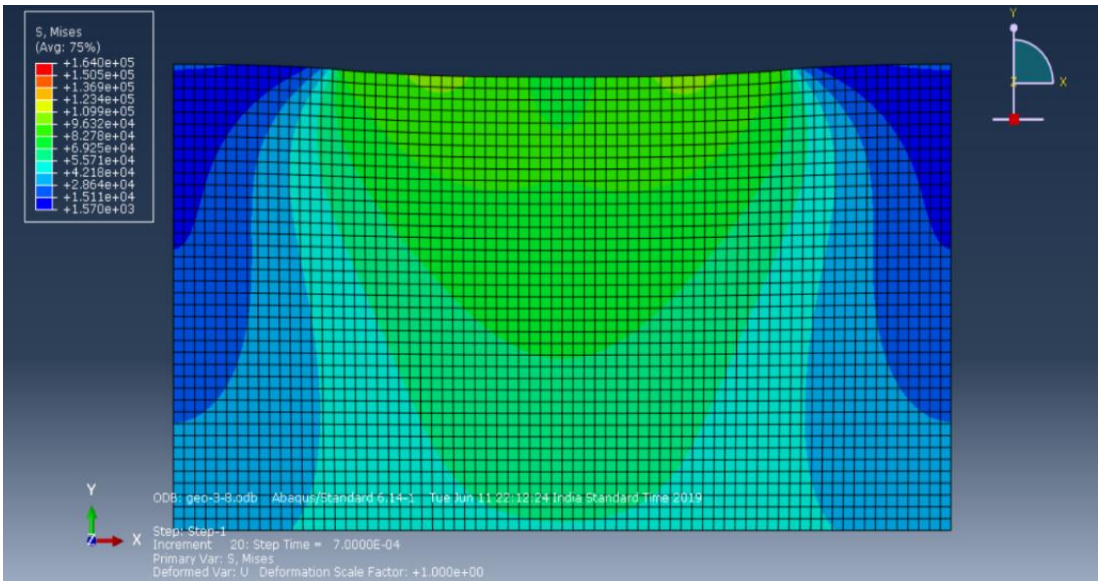

Figure 4.8 Subgrade Stress Distribution in 2-D Model with Geocell Confinement Width 3.8m

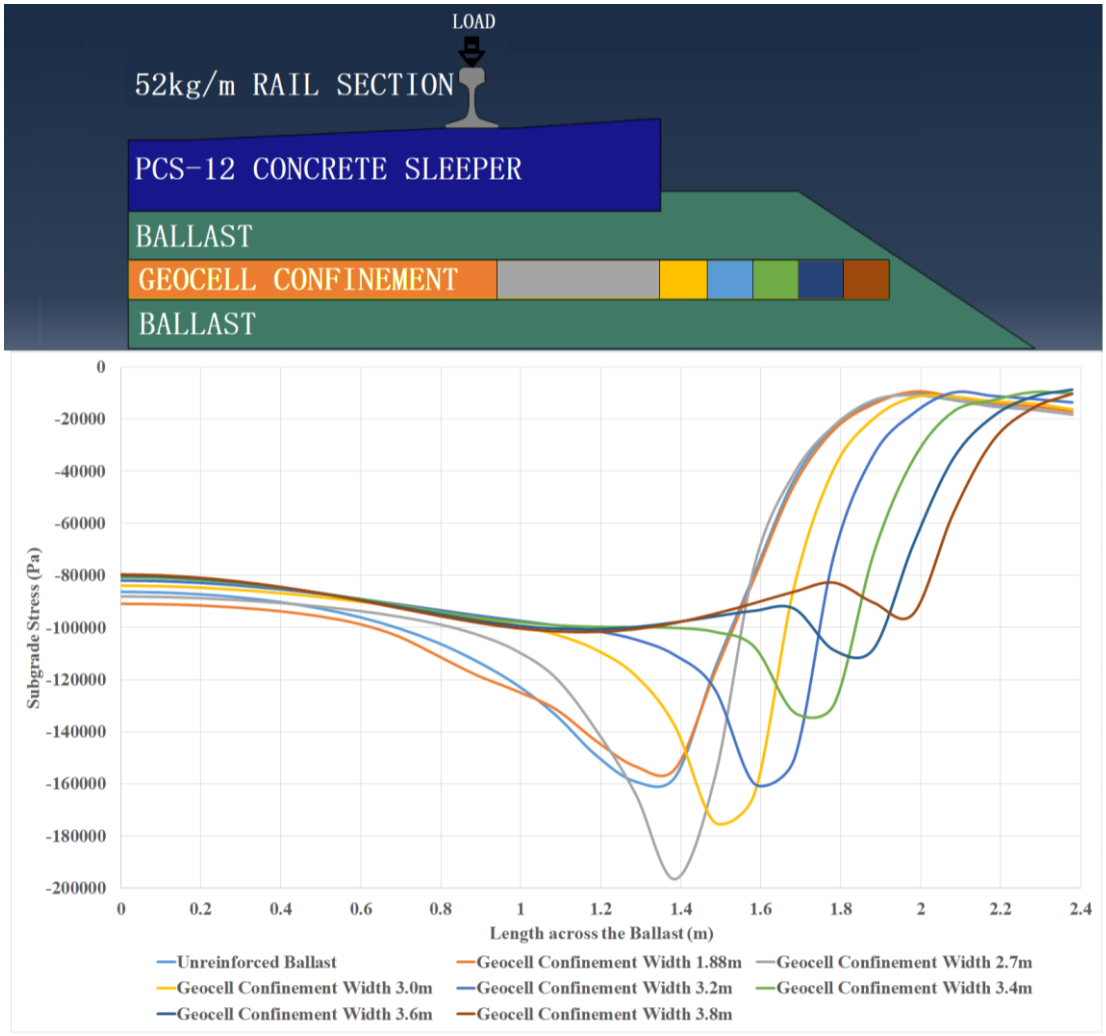

Figure 4.9 Graphical representation of Subgrade Stresses for unreinforced ballast and various Geocell Confinement Width

In Figure 4.9, accumulation of stresses can be observed at the end of geocell confinement width whose magnitude is uncertain. In the case of 2-D model analysis, stress accumulation is exaggerated. Also, unreinforced ballast model and model with geocell confinement width 1.88m behaved almost similarly in distributing stresses over the subgrade. Due to discrepancies in 2-D models, for further studies the result of the 2-D analysis will not be considered.

From the results of numerical analysis of 3-D models, stress distribution contour was plotted. Figure 4.10 to Figure 4.33 shows stress distribution contour in different views – isometric, top and section cut isometric view. For each 3-D model, all three above mentioned views are shown in the following figures.

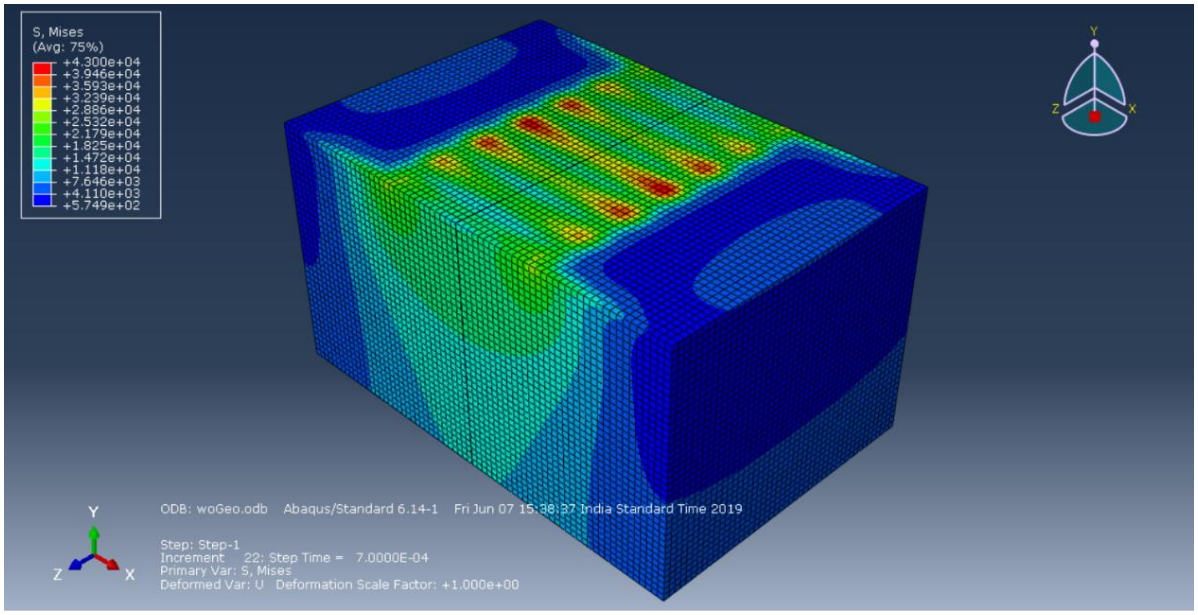

Figure 4.10 Subgrade Stress Distribution in 3-D Model with Unreinforced Ballast (Isometric View)

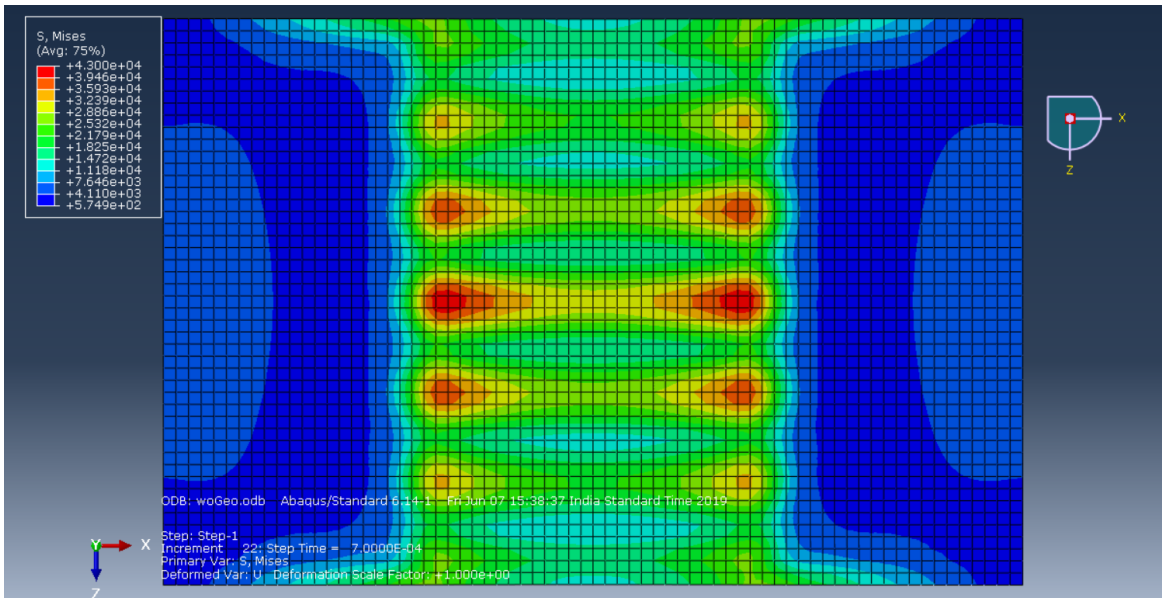

Figure 4.11 Subgrade Stress Distribution in 3-D Model with Unreinforced Ballast (Top View)

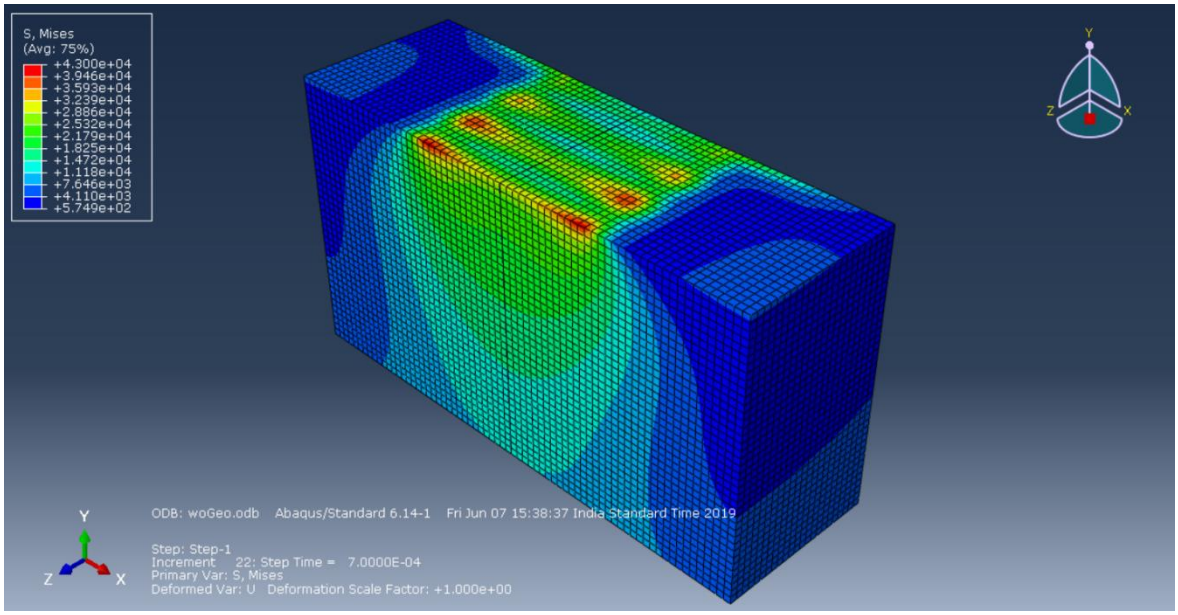

Figure 4.12 Subgrade Stress Distribution in 3-D Model with Unreinforced Ballast (Section-Cut Isometric View)

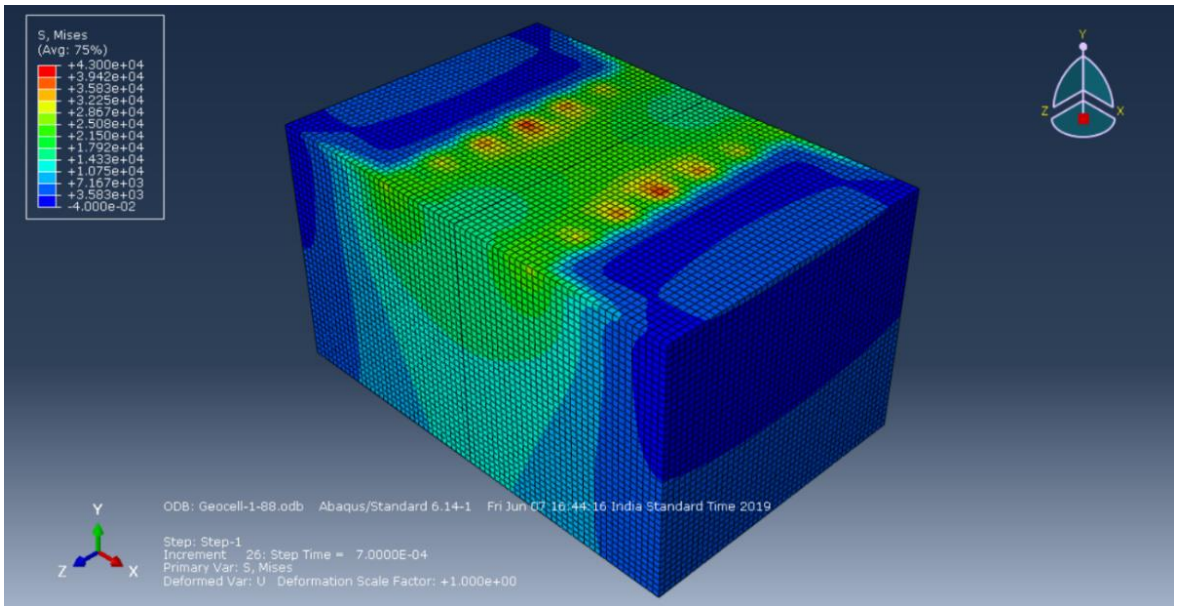

Figure 4.13 Subgrade Stress Distribution in 2-D Model with Geocell Confinement Width 1.88m (Isometric View)

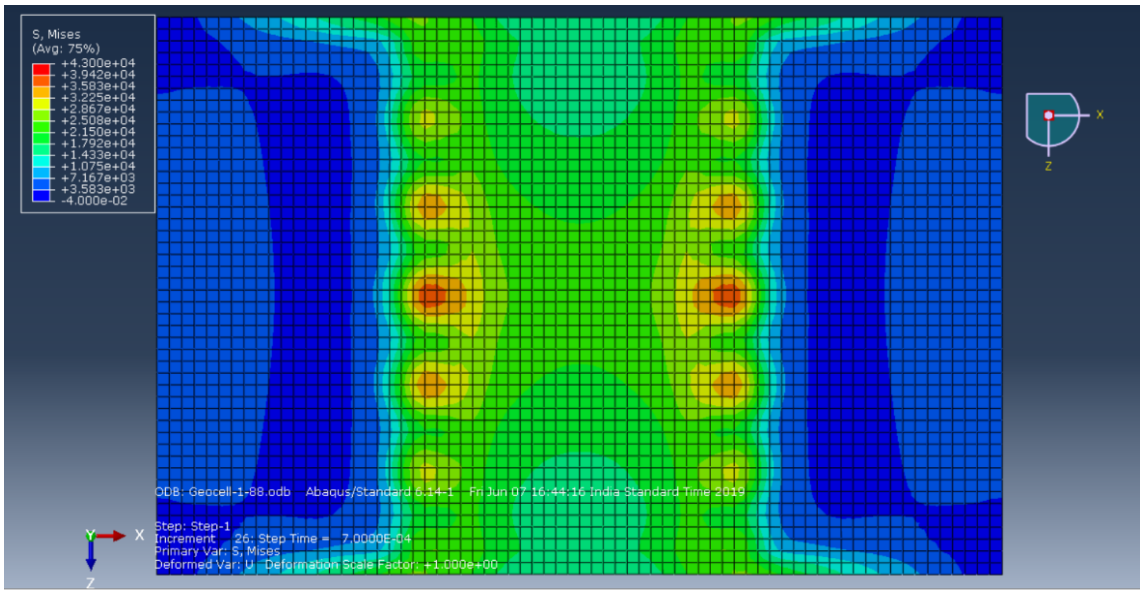

Figure 4.14 Subgrade Stress Distribution in 3-D Model with Geocell Confinement Width 1.88m (Top View)

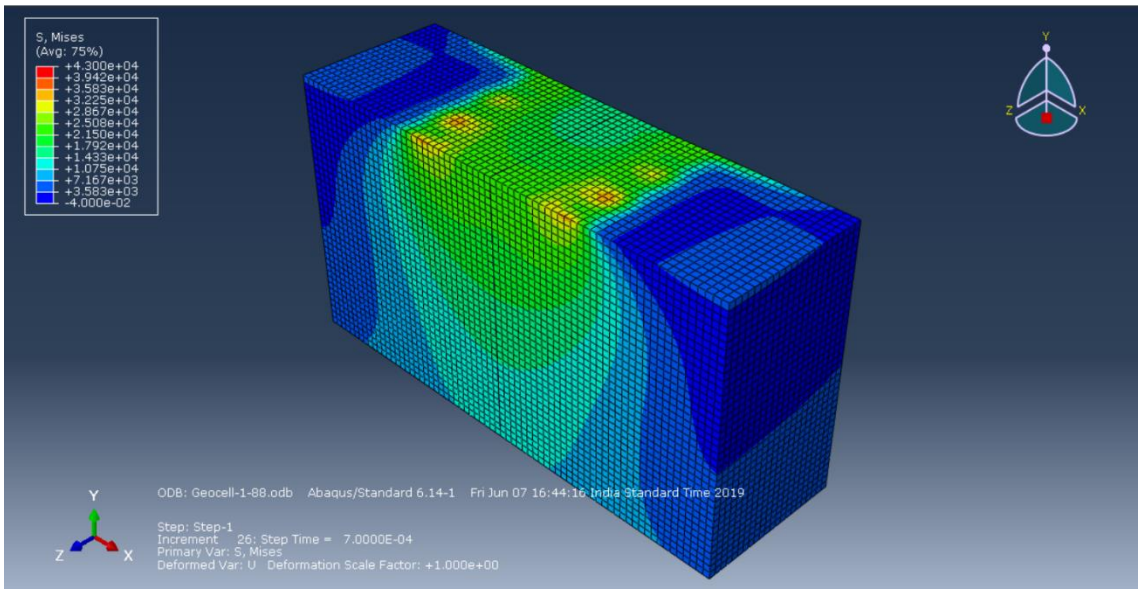

Figure 4.15 Subgrade Stress Distribution in 3-D Model with Geocell Confinement Width 1.88m (Section-Cut Isometric View)

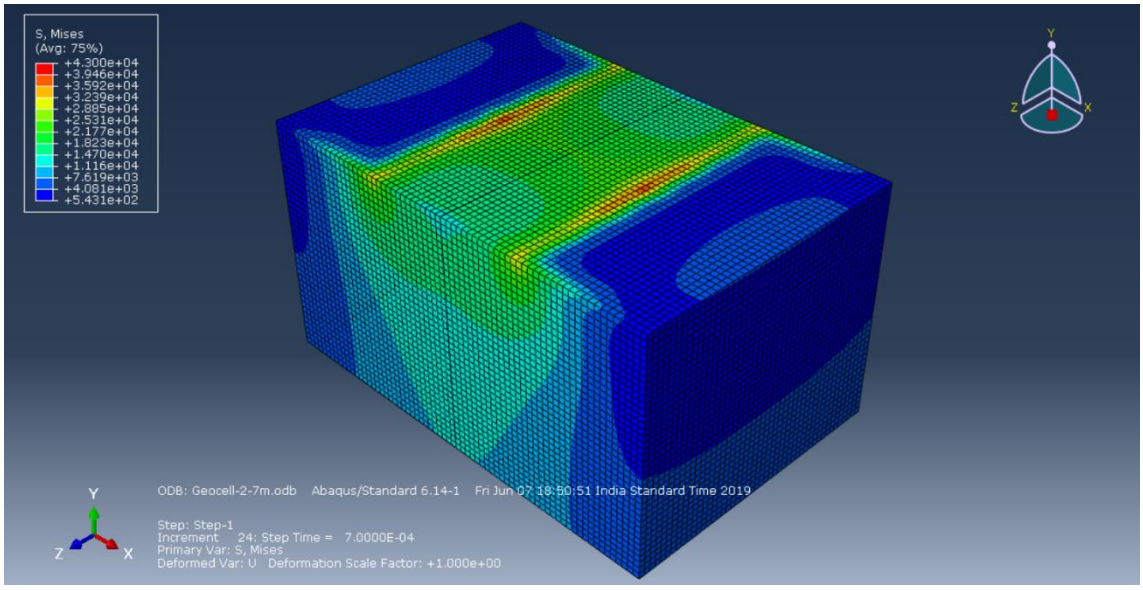

Figure 4.16 Subgrade Stress Distribution in 3-D Model with Geocell Confinement Width 2.70m (Isometric View)

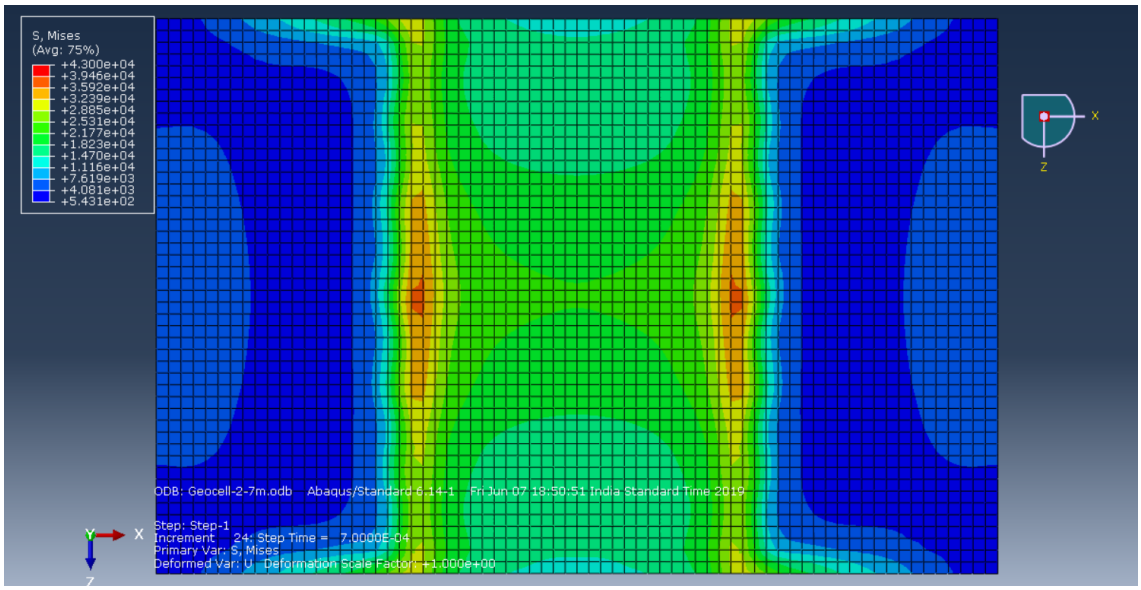

Figure 4.17 Subgrade Stress Distribution in 3-D Model with Geocell Confinement Width 2.70m (Top View)

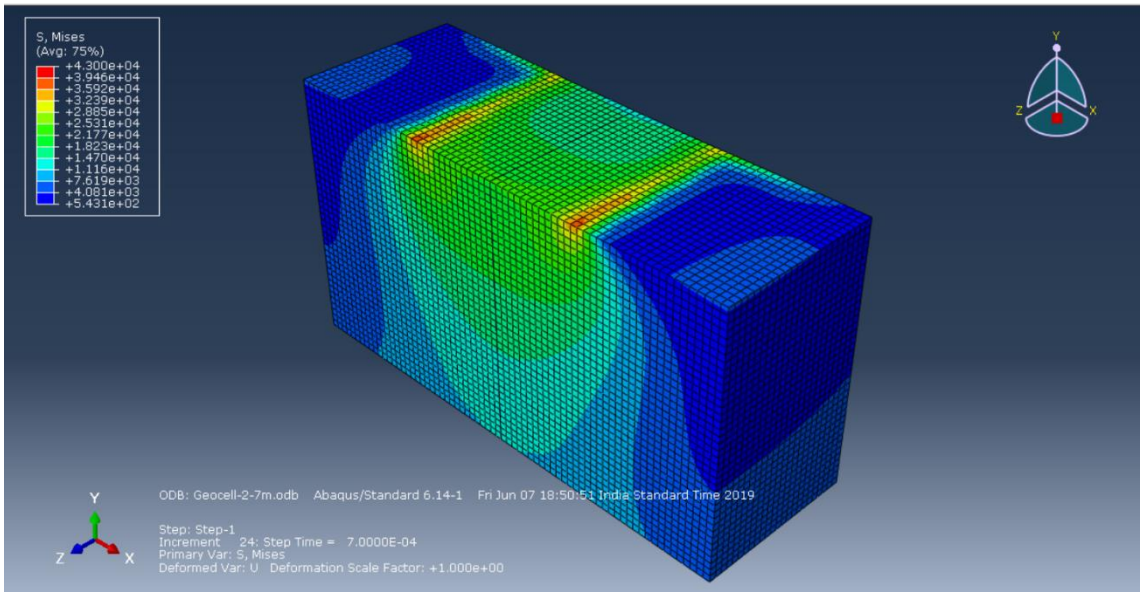

Figure 4.18 Subgrade Stress Distribution in 3-D Model with Geocell Confinement Width 2.70m (Section-Cut Isometric View)

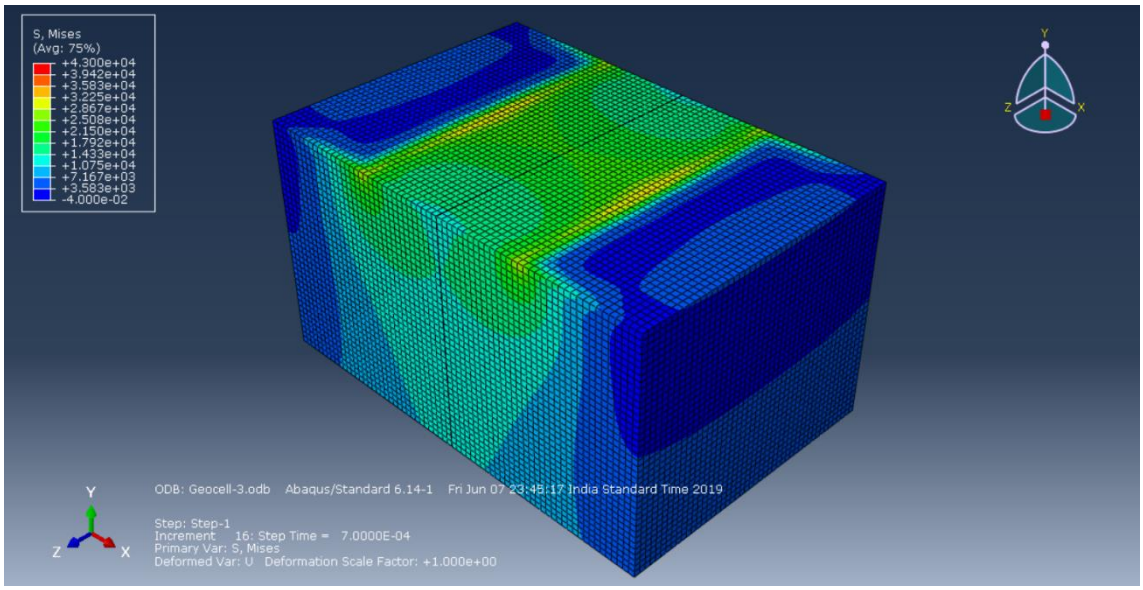

Figure 4.19 Subgrade Stress Distribution in 3-D Model with Geocell Confinement Width 3.0m (Isometric View)

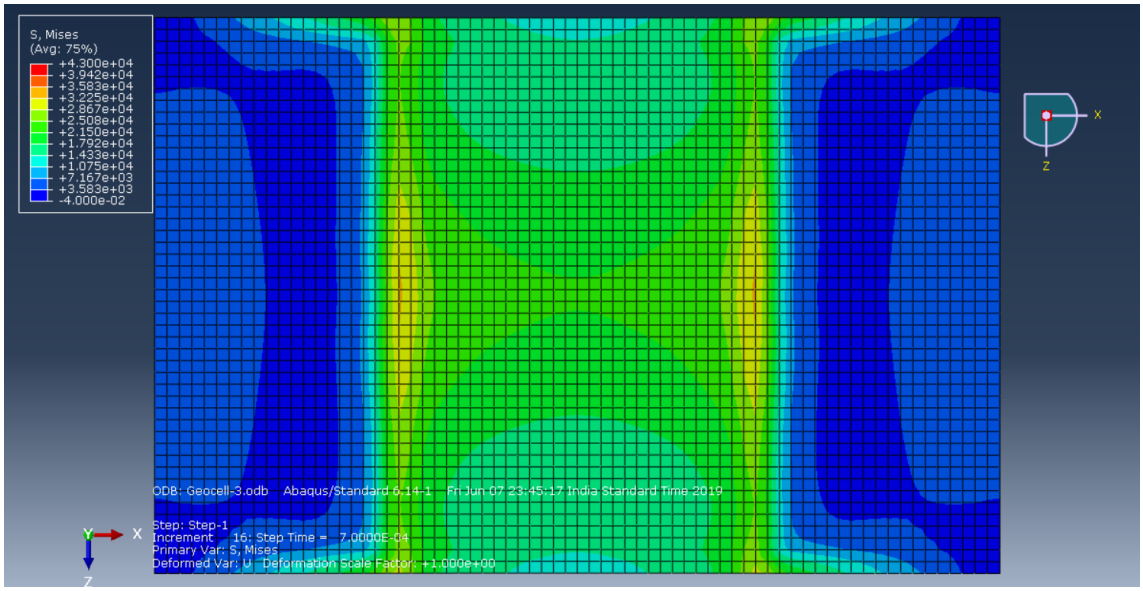

Figure 4.20 Subgrade Stress Distribution in 3-D Model with Geocell Confinement Width 3.0m (Top View)

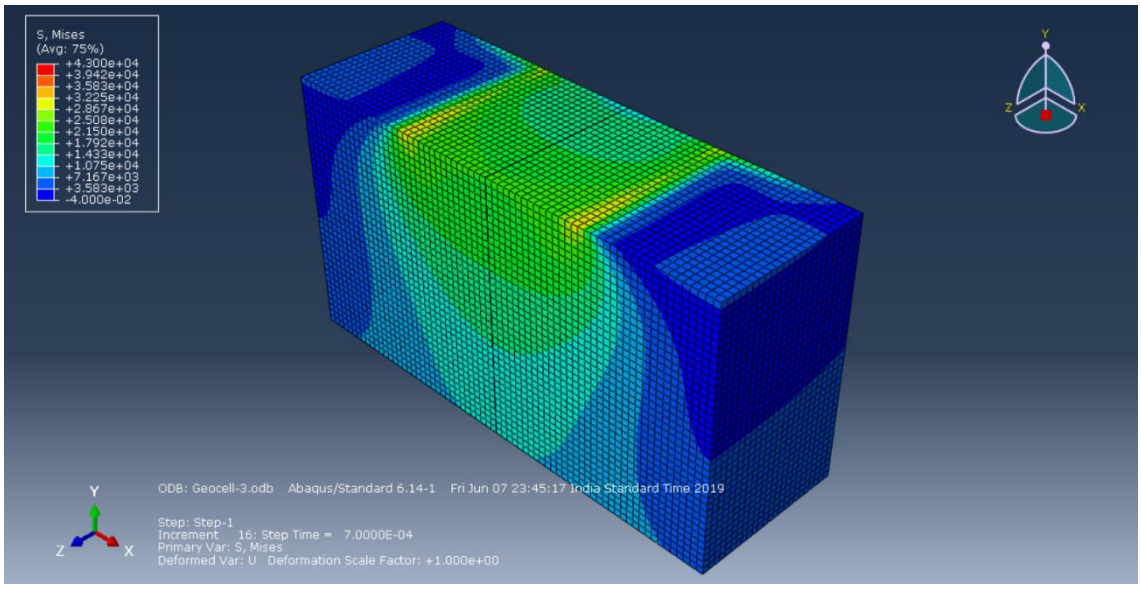

Figure 4.21 Subgrade Stress Distribution in 3-D Model with Geocell Confinement Width 3.0m (Section-Cut Isometric View)

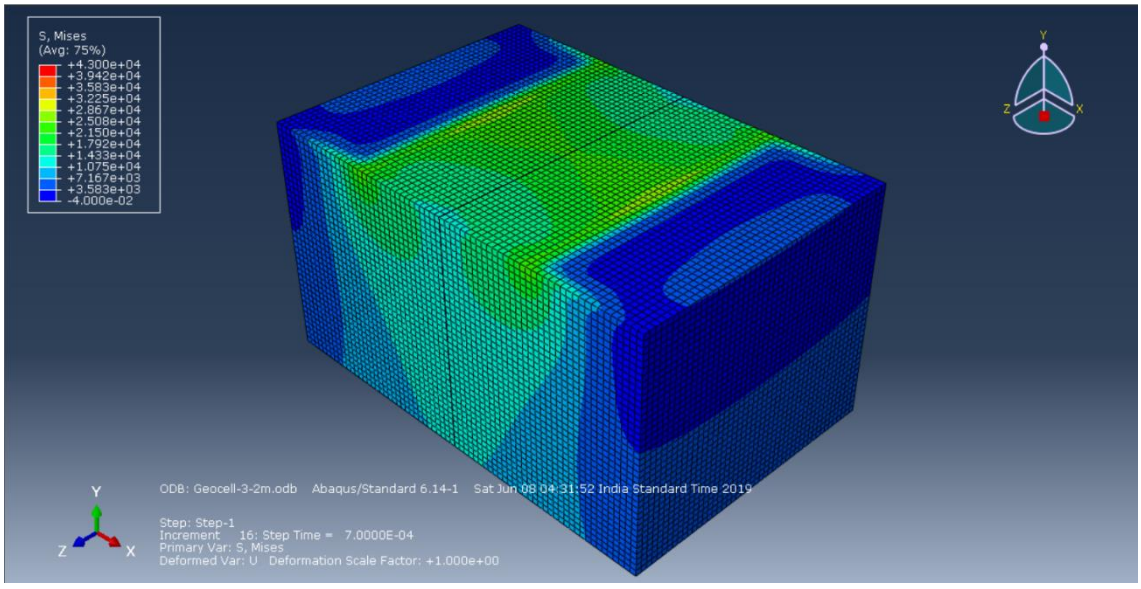

Figure 4.22 Subgrade Stress Distribution in 3-D Model with Geocell Confinement Width 3.2m (Isometric View)

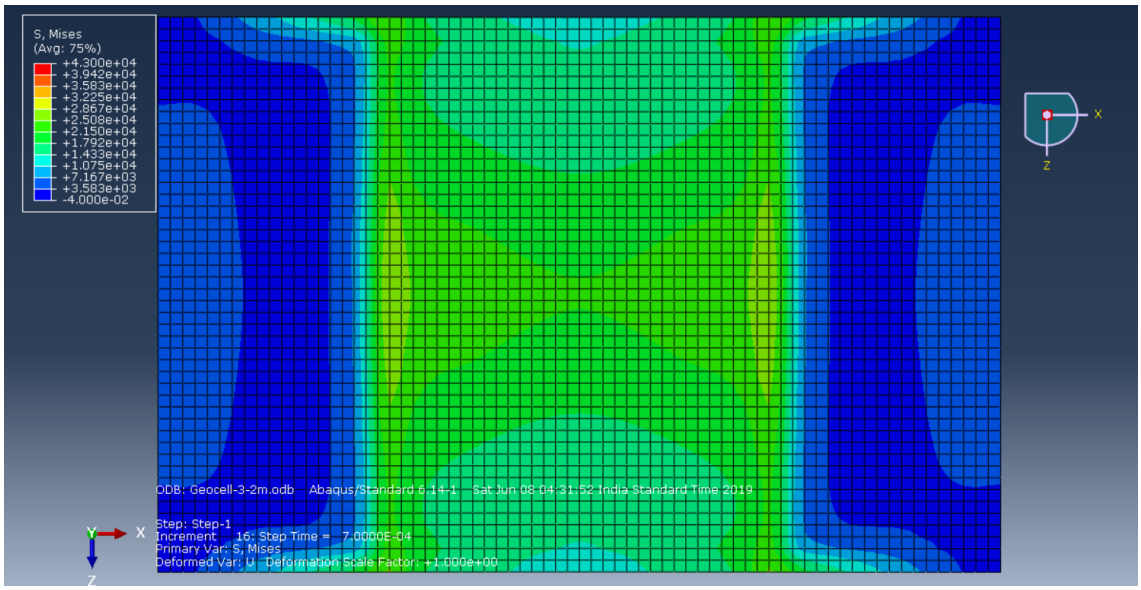

Figure 4.23 Subgrade Stress Distribution in 3-D Model with Geocell Confinement Width 3.2m (Top View)

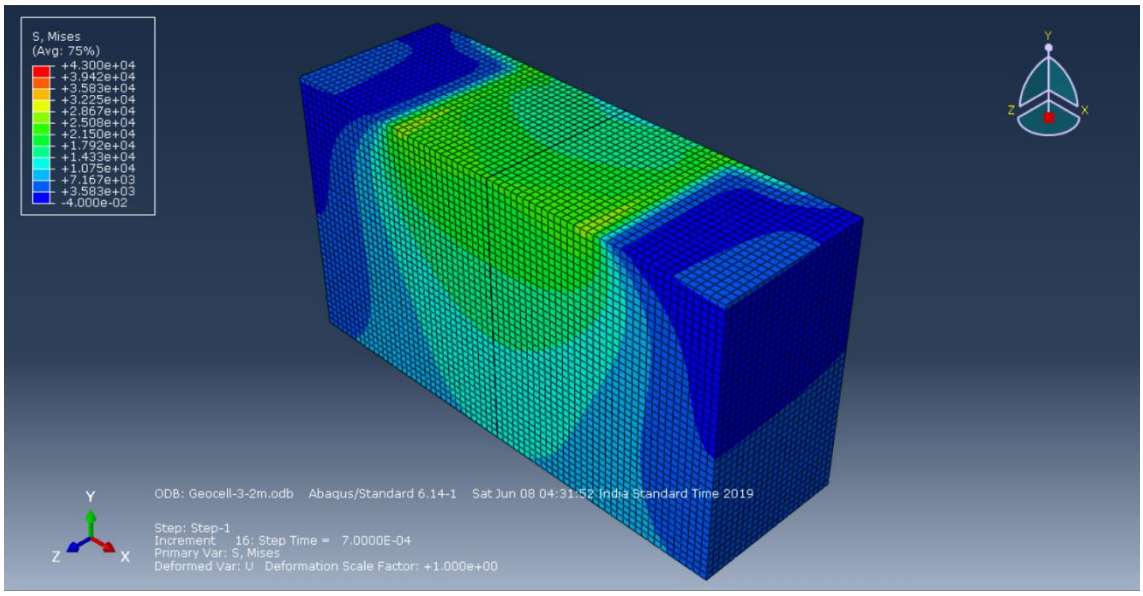

Figure 4.24 Subgrade Stress Distribution in 3-D Model with Geocell Confinement Width 3.2m (Section-Cut Isometric View)

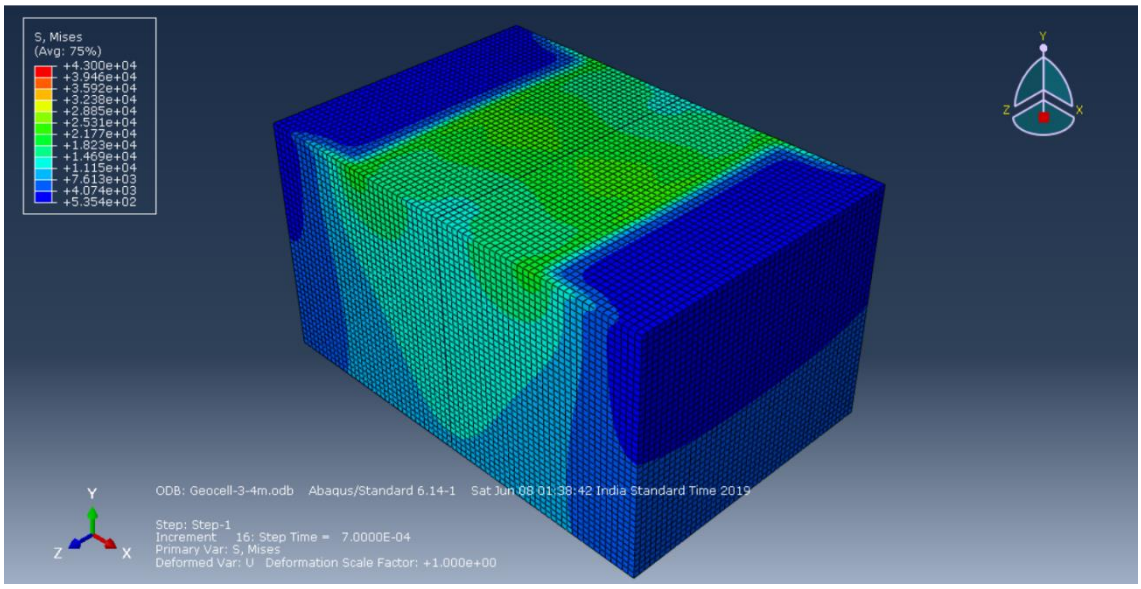

Figure 4.25 Subgrade Stress Distribution in 3-D Model with Geocell Confinement Width 3.4m (Isometric View)

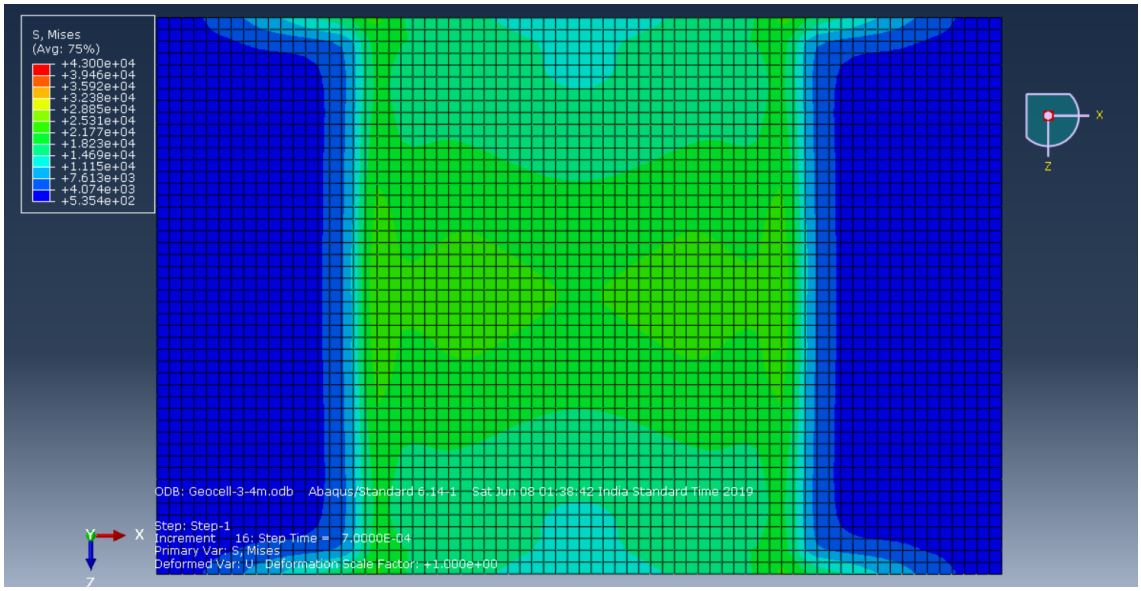

Figure 4.26 Subgrade Stress Distribution in 3-D Model with Geocell Confinement Width 3.4m (Top View)

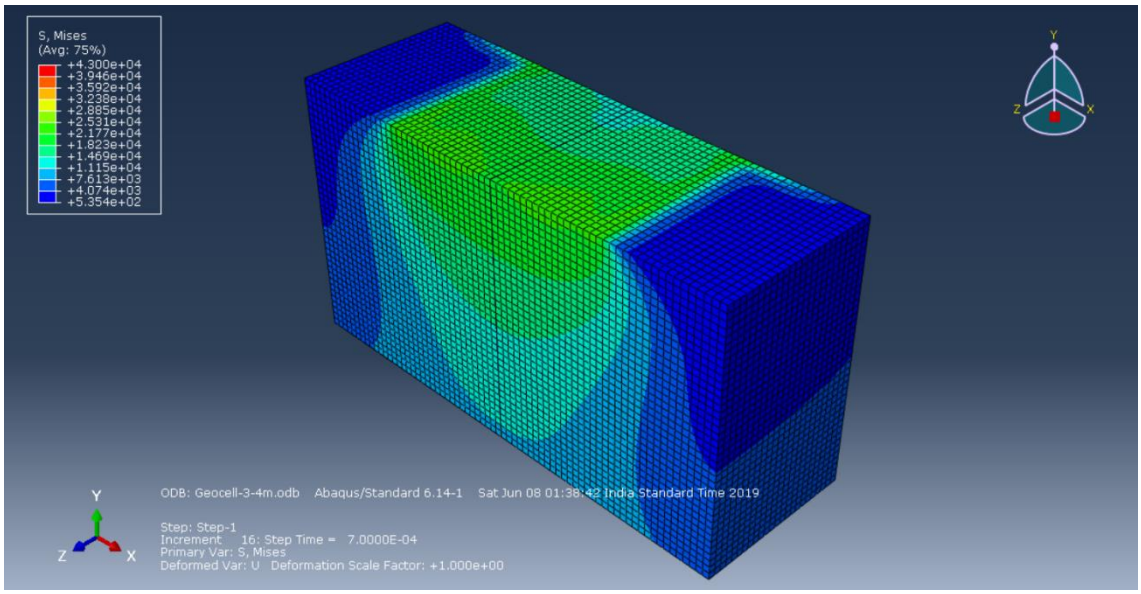

Figure 4.27 Subgrade Stress Distribution in 3-D Model with Geocell Confinement Width 3.4m (Section-Cut Isometric View)

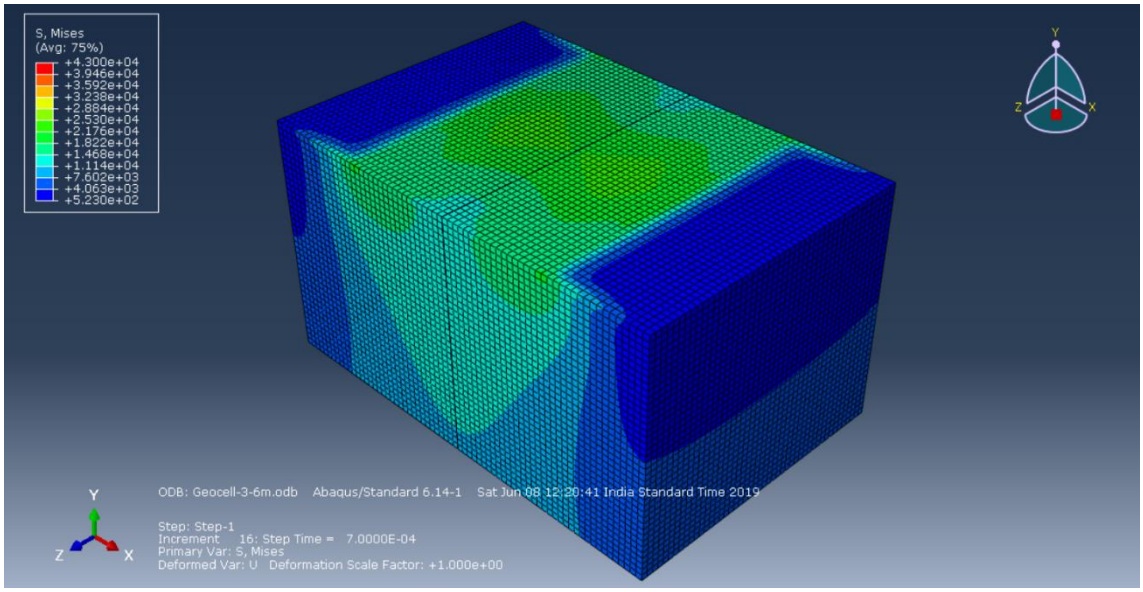

Figure 4.28 Subgrade Stress Distribution in 3-D Model with Geocell Confinement Width 3.6m (Isometric View)

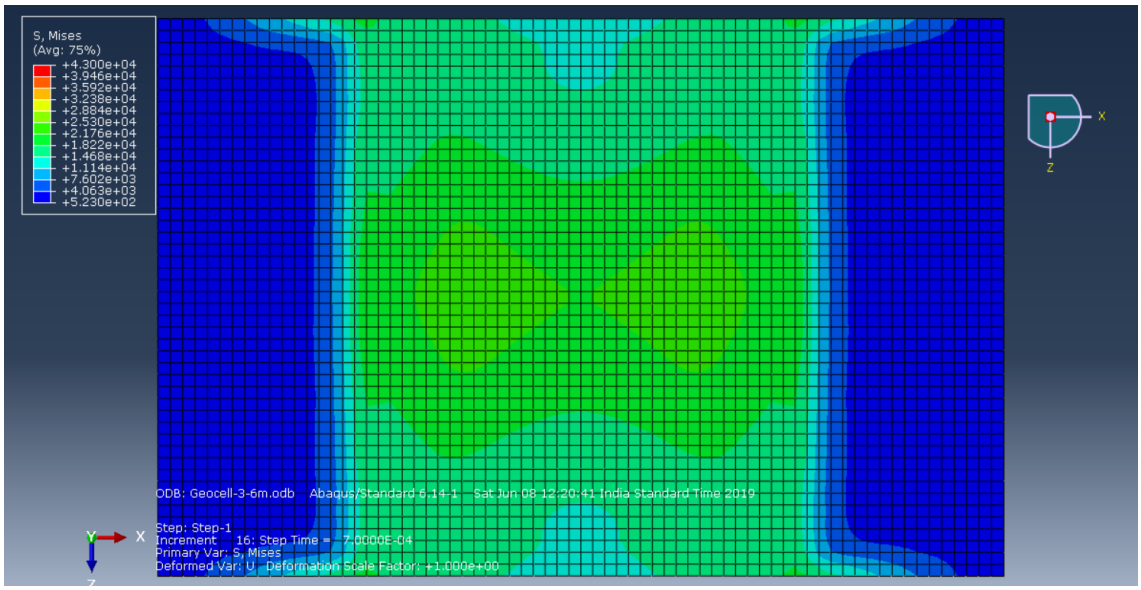

Figure 4.29 Subgrade Stress Distribution in 3-D Model with Geocell Confinement Width 3.6m (Top View)

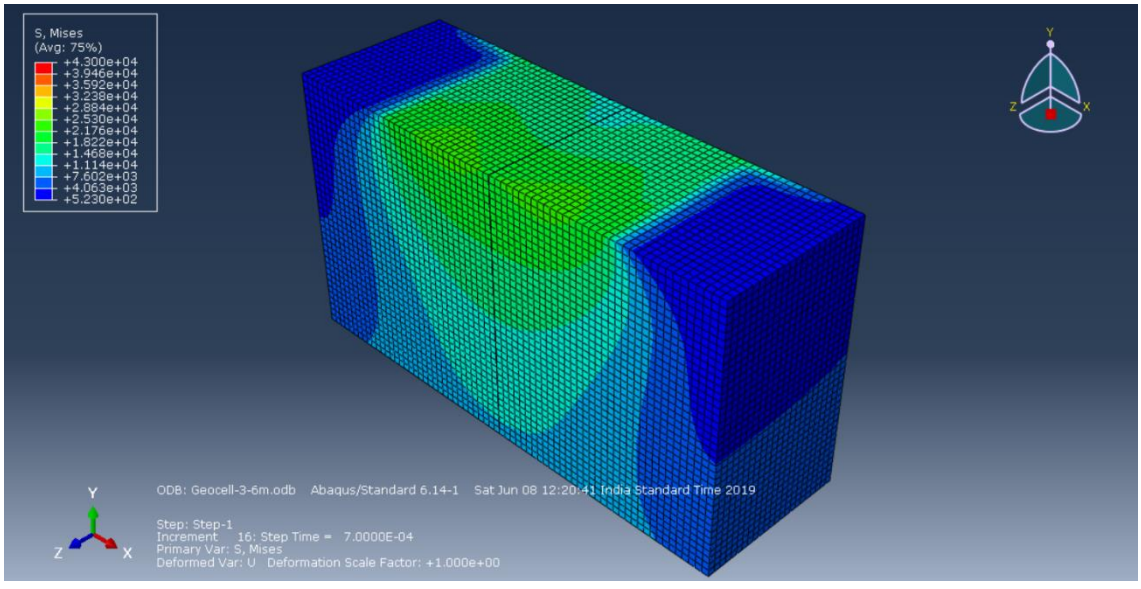

Figure 4.30 Subgrade Stress Distribution in 3-D Model with Geocell Confinement Width 3.6m (Section-Cut Isometric View)

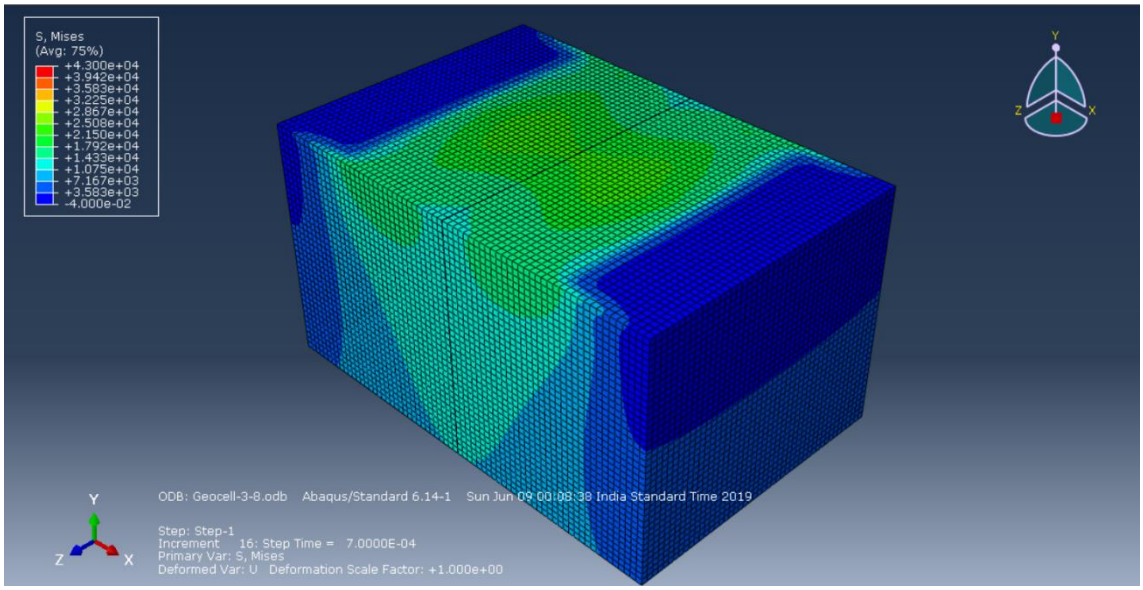

Figure 4.31 Subgrade Stress Distribution in 3-D Model with Geocell Confinement Width 3.8m (Isometric View)

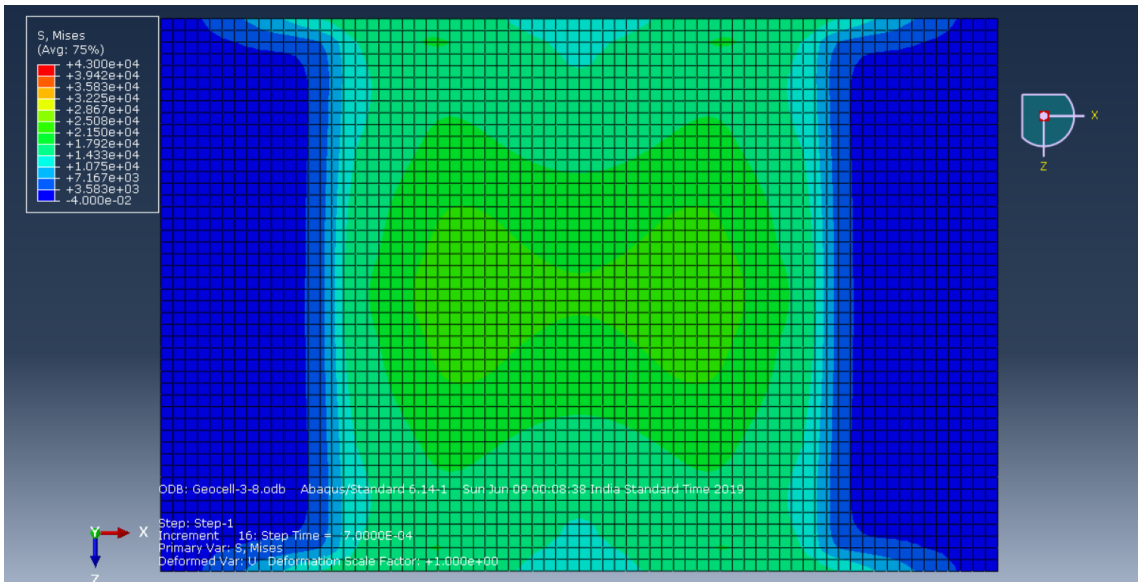

Figure 4.32 Subgrade Stress Distribution in 3-D Model with Geocell Confinement Width 3.8m (Top View)

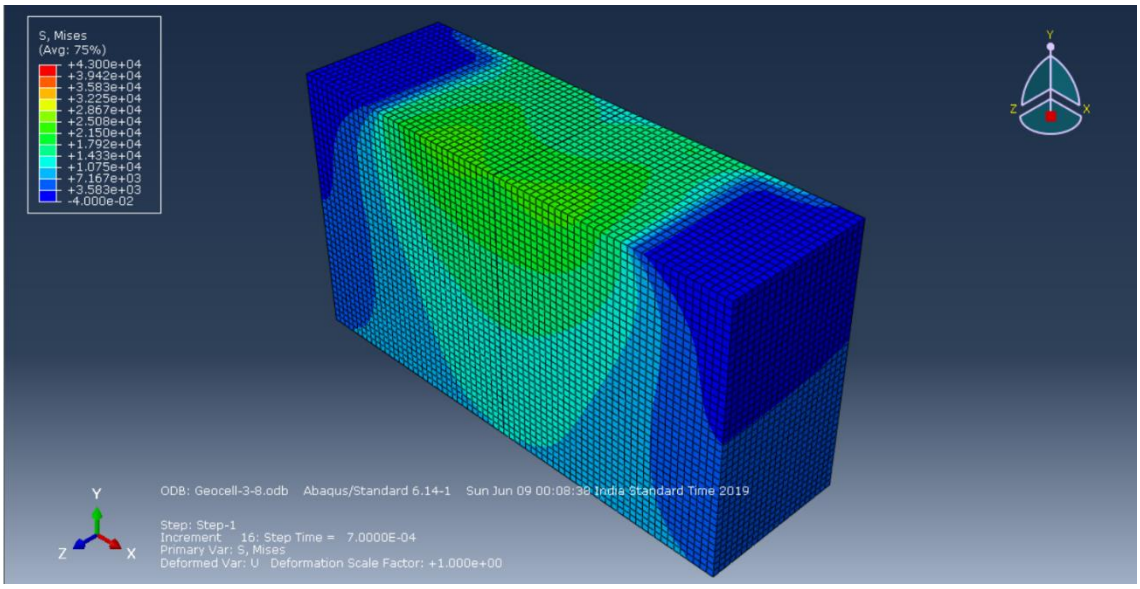

Figure 4.33 Subgrade Stress Distribution in 3-D Model with Geocell Confinement Width 3.8m (Section-Cut Isometric View)

From Figure 4.10 to Figure 4.33, it can be observed on the inclusion of geocell confinement uniforms the stress distribution and increase in its width decreases the subgrade stress, in each view. For more precision in results, stresses at a depth of 0.1 m form subgrade surface were calculated in each case and the comparison graph was plotted as shown in Figure 4.34

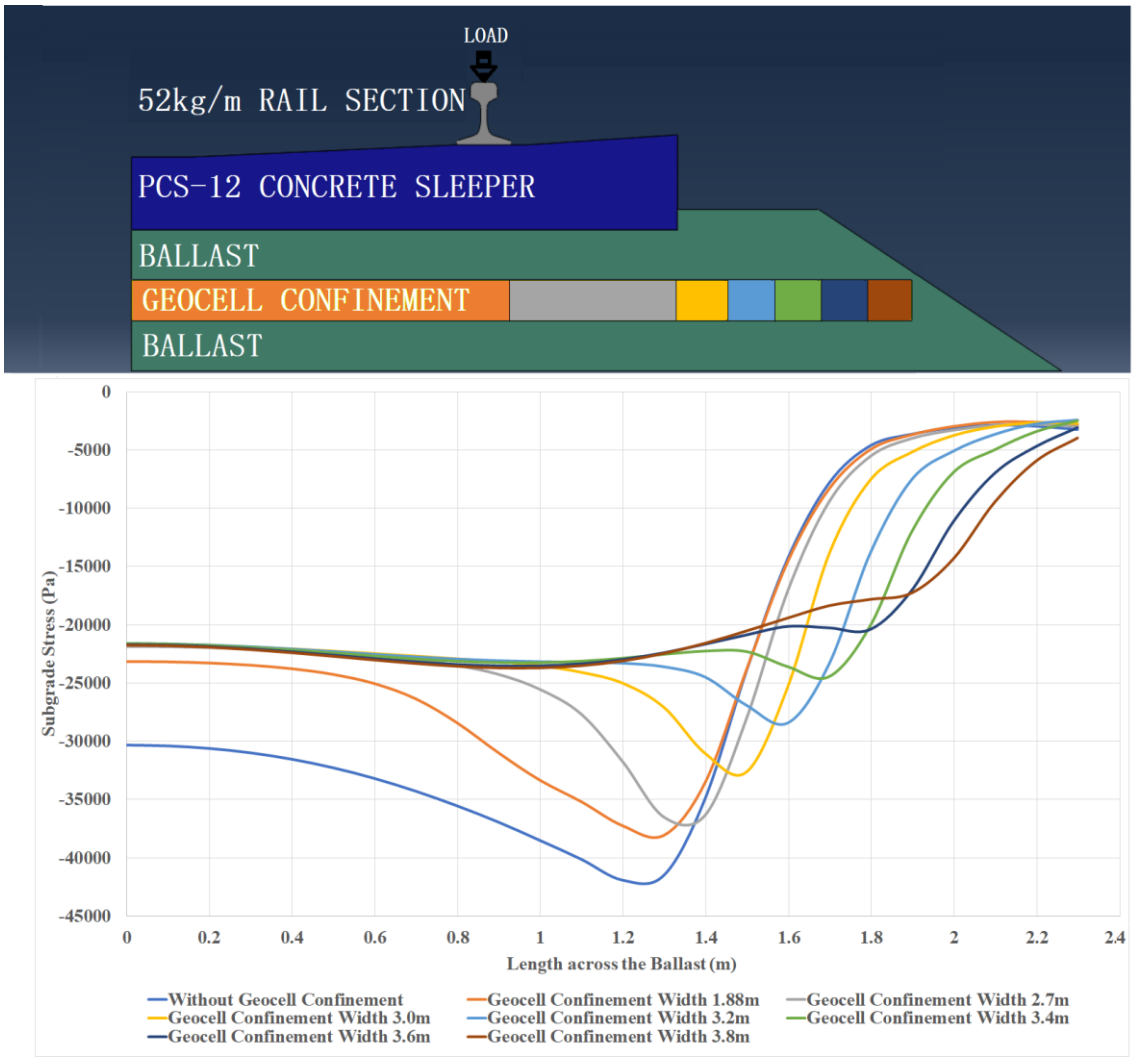

Figure 4.34 Comparison of Subgrade Stresses over the length across the Ballast for different Geocell Confinement

Similarly, the graph was plotted for subgrade stress along the length of the rail at the same depth from the subgrade surface, shown in Figure 4.35. Also stresses in ballast slopped surface were plotted in the comparison graph as shown in Figure 4.36.

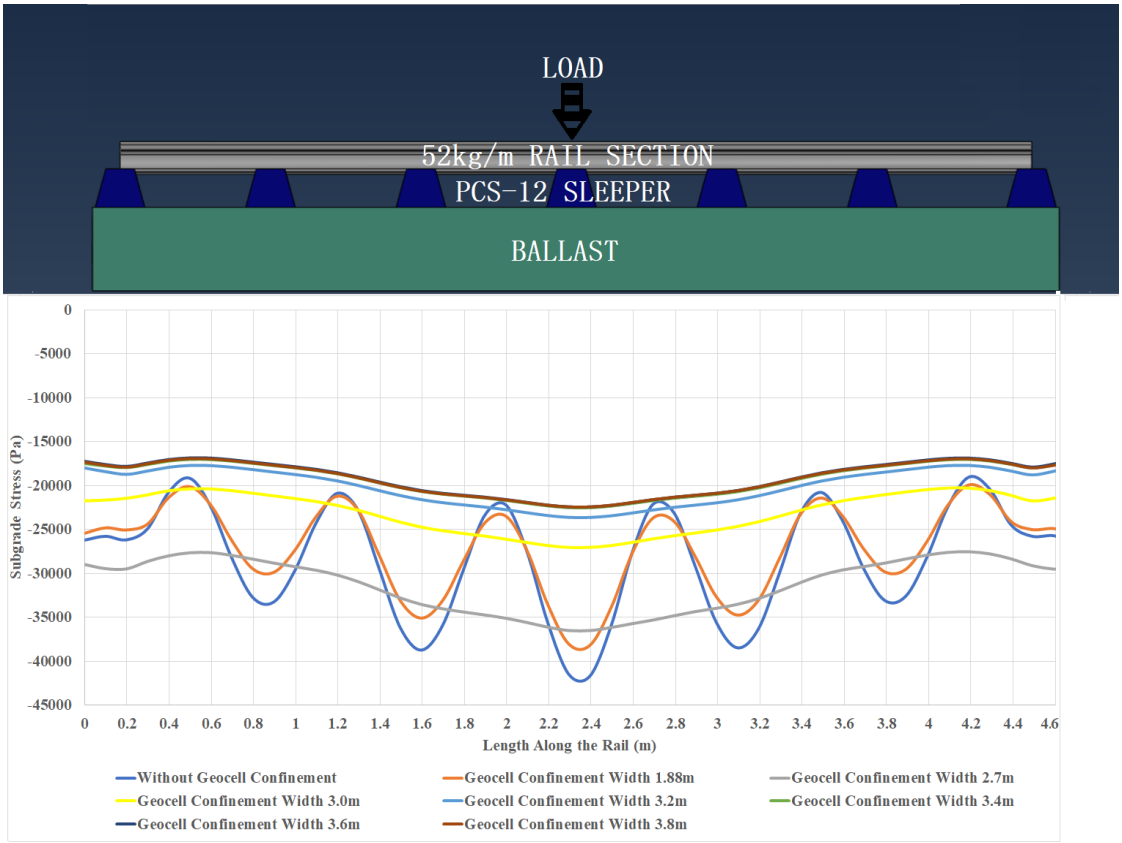

Figure 4.35 Comparison of Subgrade Stresses over the length along the Rail for different Geocell Confinement

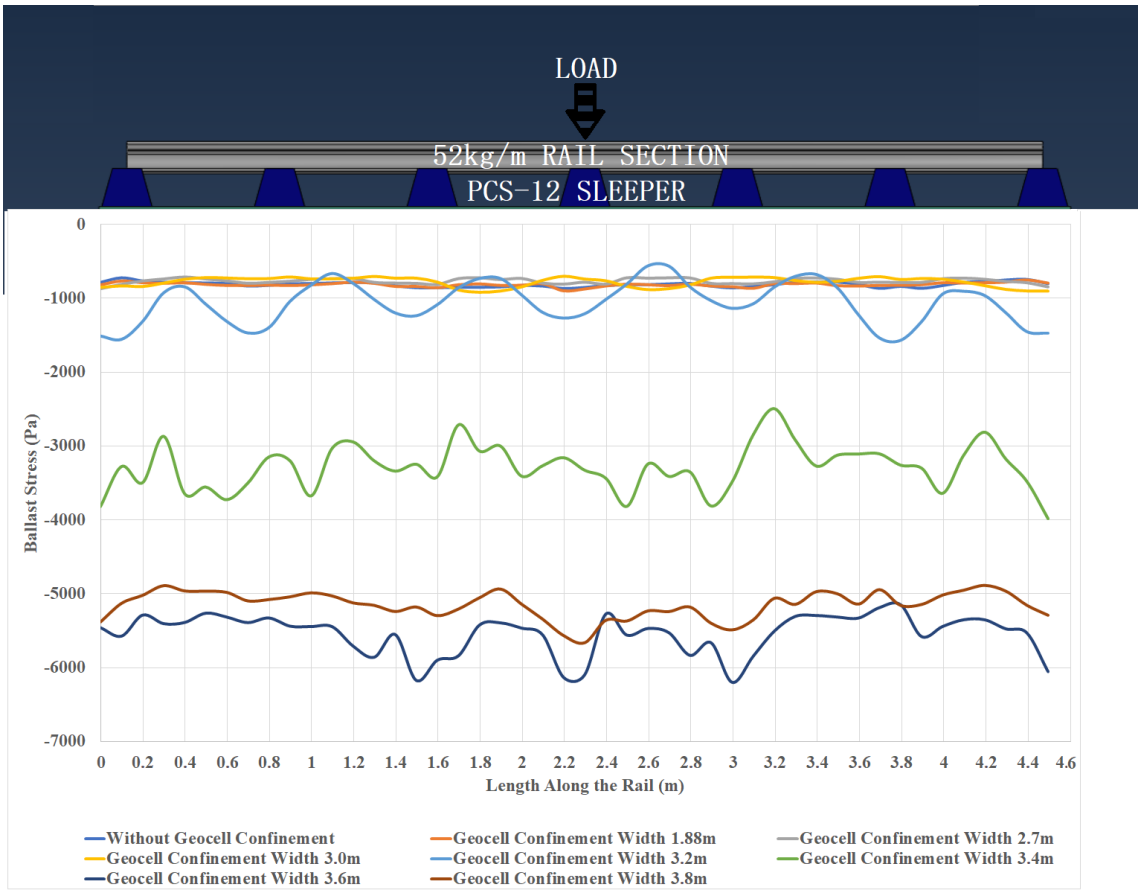

Figure 4.36 Comparison of Ballast Stresses over the Ballast Slope Surface for different Geocell Confinement

From Figure 4.34 and Figure 3.35, it was observed that as geocell confinement width increases stress along the rail and across the ballast decreases. Maximum subgrade stress in model with unreinforced ballast is 41941.29 Pa and Table 4.1 shows maximum subgrade stress in different cases and percentage improvement in stress distribution with respect to model with unreinforced ballast. It can be observed that as the width of geocell confinement increases, maximum subgrade stress decreases. The magnitude incremental percentage decrease in maximum subgrade stress for confinement width greater than 3.40m.

Table 4.1 Maximum subgrade stresses in numerical models

3-D Model	Maximum Subgrade Stress (Pa)	Percentage decrease in Maximum Subgrade Stress (%)	Incremental percentage decrease in Maximum Subgrade Stress (%)
Geocell Confinement Width 1.88m	38078.05	9.21	-
Geocell Confinement Width 2.70m	36531.94	12.89	39.95
Geocell Confinement Width 3.00m	32598.57	22.27	72.7
Geocell Confinement Width 3.20m	28446.60	32.17	44.45
Geocell Confinement Width 3.40m	24474.96	41.64	29.43
Geocell Confinement Width 3.60m	23538.94	43.87	5.35
Geocell Confinement Width 3.80m	23702.23	43.48	-0.88

Also, Table 4.2 gives maximum ballast stresses on ballast slope surface and percentage increase in stresses due to the inclusion of geocell confinement. Maximum ballast stress in case of the model with unreinforced ballast is $869.58Pa$. It can be observed that increment beyond 3.0m confinement width results into a drastic increase in stress over the ballast slope surface. These increased stresses in the ballast layer especially on slopped surface of ballast may result in blowing out of granular material of ballast embankment. Therefore, width greater than 3.0m should be avoided

Table 4.2 Maximum Ballast Stress on ballast slope surface

3-D Model	Maximum Ballast Stress (Pa)	Percentage increase in stress (%)
Geocell Confinement Width 1.88m	895.90	3.02
Geocell Confinement Width 2.70m	869.97	0.04
Geocell Confinement Width 3.00m	923.25	6.17
Geocell Confinement Width 3.20m	1574.41	81.05
Geocell Confinement Width 3.40m	3989.52	358.78
Geocell Confinement Width 3.60m	6202.67	613.29
Geocell Confinement Width 3.80m	5661.97	566.19

Also, on comparing the results of 2-D models and 3-D models, subgrade stresses were decreased in both cases on the inclusion of geocell in ballast layer. But the magnitude of stresses in results of 2-D models was higher than in the case of 3-D models. This is because in the case of 2-D models all layers behave as beam instead of the slab as in case of 3-D models.

CHAPTER 5

CONCLUSIONS

After a number of simulations and plots and comparing of results of each simulation, various conclusions were drawn. All the inferences drawn from the whole numerical analysis of all sixteen models are discussed as follow: -

1) Inclusion of geocell confinement in ballast layer improves the stress distribution of the subgrade layer as geocell confined ballast has high-stress tolerance and also distributes the stresses over wider width
2) As geocell confinement width increases, while rest conditions remain the same, the magnitude of decrease in subgrade stresses increases.

The optimum width of 3.0m for geocell confinement is suggested on the basis of this numerical analysis

REFERENCES

1. Agarwal, M. M. (2017). *Indian Railway Track*, 20th Ed., Standard Publishers Distributors, Delhi.
2. Atalar, C., Shin, E. C., and Das, B. M. (2009). "Elastic modulus of granular soil-geogrid composite from cyclic plate load tests", *Proc., 17th International Conference on Soil Mechanics and Geotechnical Engineering*, Alexandria, Egypt, 2212-2215.
3. Chaney, R., Demars, K., Gabr, M. A., and Hart, J. (2000). "Elastic Modulus of Geogrid-Reinforced Sand Using Plate Load Tests." *Geotechnical Testing Journal*, 23(2), 245-250.
4. Cowland, J. W., and Wong, S. C. K. (1993). "Performance of a road embankment on soft clay supported on a Geocell mattress foundation." *Geotextiles and Geomembranes*, 12(8), 687–705.
5. Das, B. M. (2016). "Use of geogrid in the construction of railroads." *Innovative Infrastructure Solutions*, 1(15), 1-12.
6. Esmaeili, M., Naderi, B., Neyestanaki, H. K., and Khodaverdian, A. (2018). "Investigating the effect of geogrid on stabilization of high railway embankments." *Soils and Foundations*, 58(2), 319–332.
7. Fu, Q., and Zheng, C. (2014). "Three-dimensional dynamic analyses of track-embankment-ground system subjected to high speed train loads." *The Scientific World Journal*, 2014(924592), 1-12.
8. Han, J., and Gabr, M. A. (2002). "Numerical Analysis of Geosynthetic-Reinforced and Pile-Supported Earth Platforms over Soft Soil." *Journal of Geotechnical and Geoenvironmental Engineering*, 128(1), 44–53.
9. Indraratna, B., Khabbaz, H., Salim, W., and Christie, D. (2006). "Geotechnical Properties of Ballast and the Role of Geosynthetics", *Journal of Ground Improvement*, 10(3), 91-102.
10. Indraratna, B., Rujikiatkamjorn, C., Wijeyakulasuriya, V., Shahin, M. A., and Christie, D. (2006). "Soft soil stabilization under railway embankments", *Proc., Indian Geotechnical Conference*, Chennai, India, 41-50.
11. Koerner, R. M. (2005). *Designing with Geosynthetics,* 5th Ed., Prentice Hall, Upper Saddle River, New Jersey.

12. Kumar, K., and Sambasivarao, K. (2014). “Static and Dynamic Analysis of Railway Track Sleeper.” *International Journal of Engineering Research and General Science*, 2(6), 662-671.
13. Lackenby, J., Indraratna, B., McDowell, G. R., and Christie, D. (2007). "Effect of confining pressure on ballast degradation and deformation under cyclic triaxial loading." *Geotechnique*, 57(6), 527–536.
14. Lal, R., Singh, R. C., and Singh, D. (2016). "*Stress Analysis at Contact Region of Rail-Wheel: Review*." *Proc., Vth International Symposium on “Fusion of Science & Technology”*, New Delhi, India, 75-85.
15. Leshchinsky, B., and Ling, H. (2013). "Effects of Geocell Confinement on Strength and Deformation Behavior of Gravel." *Journal of Geotechnical and Geoenvironmental Engineering*, 139(2), 340–352.
16. Leshchinsky, B., Evans, T. M., and Vesper, J. (2016). "Microgrid inclusions to increase the strength and stiffness of sand." *Geotextiles and Geomembranes*, 44(2), 170–177.
17. Li, D., Hyslip, J., Ted Sussmann, T., and Chrismer, S. (2015). *Railway Geotechnics*, 1st Ed., CRC Press, Florida.
18. Mundrey, J. S. (2009). *Railway Track Engineering*, 4th Ed., Tata McGraw Hill Education, New Delhi.
19. Nikraz H, M. A., and H, N. (2015). "Bearing Capacity Evaluation of Footing on a Layered- Soil using ABAQUS. " *Journal of Earth Science & Climatic Change*, 6(3), 1-8.
20. Rajagopal, K., Krishnaswamy, N. R., and Madhavi Latha, G. (1999). "Behaviour of sand confined with single and multiple geocells." *Geotextiles and Geomembranes*, 17(3), 171–184.
21. Smith, M. (2014). *ABAQUS/Standard User's Manual*, Version 6.14, Simulia, Rhode Island.
22. Srinivasan, M. (1969). *Modern permanent way*, 1st Ed., Somaiya Publications, Mumbai.
23. Van Dyk, B. J., Edwards, J. R., Dersch, M. S., Ruppert, C. J., and Barkan, C. P. (2017). "Evaluation of dynamic and impact wheel load factors and their application in design processes. " *Proc.,Institution of Mechanical Engineers, Journal of Rail and Rapid Transit*, London, England, 231(1), 33–43.

24. Yetimoglu, T., Wu, J. T. H., and Saglamer, A. (1994). "Bearing Capacity of Rectangular Footings on Geogrid- Reinforced Sand." *Journal of Geotechnical Engineering*, 120(12), 2083–2099.
25. Zhou, H., and Wen, X. (2008). "Model studies on geogrid- or geocell-reinforced sand cushion on soft soil." *Geotextiles and Geomembranes*, 26(3), 231–238.
26. Ziaie, R. (2011). "Effect of Utilization of Geosynthetic on reducing the required thickness of sub-base layer of two layered soil", *International Journal of Geological and Environmental Engineering*, 5(1), 27-31.

NUMERICAL MODELLING FOR STRESSES IN RAILWAY SUBGRADE WITH GEOCELL CONFINED BALLAST

ORIGINALITY REPORT

7%	1%	4%	4%
SIMILARITY INDEX	INTERNET SOURCES	PUBLICATIONS	STUDENT PAPERS

PRIMARY SOURCES

1	Hu, J.C.. "An interpretation of the active deformation of southern Taiwan based on numerical simulation and GPS studies", Tectonophysics, 19970615 Publication	2%
2	Santosh Chavan, Veershetty Gumtapure, D. Arumuga Perumal. "Computational investigation of bounded domain with different orientations using CPCM", Journal of Energy Storage, 2019 Publication	1%
3	Submitted to University of Sheffield Student Paper	1%
4	Qiang Fu, Changjie Zheng. "Three-Dimensional Dynamic Analyses of Track-Embankment-Ground System Subjected to High Speed Train Loads", The Scientific World Journal, 2014 Publication	<1%
5	as.nida.ac.th Internet Source	

		<1%
6	Submitted to University of Wollongong Student Paper	<1%
7	zolodoc.com Internet Source	<1%
8	etd.lsu.edu Internet Source	<1%
9	Submitted to University of Newcastle upon Tyne Student Paper	<1%
10	Dimitrios Papanikolaou. "The effect of geological anisotropies on the detectability of seismic electric signals", Tectonophysics, 1993 Publication	<1%
11	"Recent Advances in QSAR Studies", Springer Science and Business Media LLC, 2010 Publication	<1%
12	Kok Keng Ang, Jian Dai. "Response analysis of high-speed rail system accounting for abrupt change of foundation stiffness", Journal of Sound and Vibration, 2013 Publication	<1%
13	Submitted to Universiti Teknologi MARA Student Paper	<1%

14	es.scribd.com Internet Source	<1%
15	Submitted to Swinburne University of Technology Student Paper	<1%
16	Saadeghvaziri, M.A.. "Seismic behavior and capacity/demand analyses of three multi-span simply supported bridges", Engineering Structures, 200801 Publication	<1%
17	Submitted to Michigan Technological University Student Paper	<1%
18	Submitted to National Institute of Technology, Hamirpur Student Paper	<1%
19	www.ejge.com Internet Source	<1%
20	www.archsd.gov.hk Internet Source	<1%

Exclude quotes	On	Exclude matches	< 10 words
Exclude bibliography	On		